



## Insight into the Last Glacial Maximum climate and environments of the Baikal region

PAVEL E. TARASOV , BORIS P. ILYASHUK, CHRISTIAN LEIPE, STEFANIE MÜLLER, BIRGIT PLESSEN, PHILIPP HOELZMANN, SVETLANA S. KOSTROVA, ELENA V. BEZRUKOVA AND HANNO MEYER

### BOREAS



Tarasov, P. E., Ilyashuk, B. P., Leipe, C., Müller, S., Plessen, B., Hoelzmann, P., Kostrova, S. S., Bezrukova, E. V. & Meyer, H.: Insight into the Last Glacial Maximum climate and environments of the Baikal region. *Boreas*. <https://doi.org/10.1111/bor.12330>. ISSN 0300-9483.

This study presents a multi-proxy record from Lake Kotokel in the Baikal region at decadal-to-multidecadal resolution and provides a reconstruction of terrestrial and aquatic environments in the area during a 2000-year interval of globally harsh climate often referred to as the Last Glacial Maximum (LGM). The studied lake is situated near the eastern shoreline of Lake Baikal, in a climatically sensitive zone that hosts boreal taiga and cold deciduous forests, cold steppe associations typical for northern Mongolia, and mountain tundra vegetation. The results provide a detailed picture of the period in focus, indicating (i) a driest phase (*c.* 24.0–23.4 cal. ka BP) with low precipitation, high summer evaporation, and low lake levels, (ii) a transitional interval of unstable conditions (*c.* 23.4–22.6 cal. ka BP), and (iii) a phase (*c.* 22.6–22.0 cal. ka BP) of relatively high precipitation (and moisture availability) and relatively high lake levels. One hotly debated issue in late Quaternary research is regional summer thermal conditions during the LGM. Our chironomid-based reconstruction suggests at least 3.5 °C higher than present summer temperatures between *c.* 22.6 and 22.0 cal. ka BP, which are well in line with warmer and wetter conditions in the North Atlantic region inferred from Greenland ice-cores. Overall, it appears that environments in central Eurasia during the LGM were affected by much colder than present winter temperatures and higher than present summer temperatures, although the effects of temperature oscillations were strongly influenced by changes in humidity.

*Pavel E. Tarasov (ptarasov@zedat.fu-berlin.de), Christian Leipe and Stefanie Müller, Institute of Geological Sciences, Paleontology, Freie Universität Berlin, Malteserstr. 74-100, Building D, Berlin D-12249, Germany; Boris P. Ilyashuk, Institute of Ecology, University of Innsbruck, Technikerstr. 25, Innsbruck A-6020, Austria; Boris P. Ilyashuk, Institute for Alpine Environment Eurac Research, Drususallee 1, Bozen/Bolzano 39100, Italy; Birgit Plessen, Helmholtz Zentrum Potsdam, Deutsches GeoForschungsZentrum, Sektion 5.2, Telegrafenberg C327, Potsdam D-14473, Germany; Philipp Hoelzmann, Institute of Geographical Sciences, Physical Geography, Freie Universität Berlin, Malteserstr. 74-100, Building B, Berlin D-12249, Germany; Svetlana S. Kostrova and Elena V. Bezrukova, A.P. Vinogradov Institute of Geochemistry, Siberian Branch of Russian Academy of Sciences, Irkutsk 664033, Russia; Svetlana S. Kostrova and Hanno Meyer, Alfred Wegener Institute for Polar and Marine Research, Research Unit Potsdam, Telegrafenberg A43, Potsdam D-14473, Germany; Elena V. Bezrukova, Institute of Archaeology and Ethnography, Siberian Branch of Russian Academy of Sciences, Novosibirsk 630090, Russia; received 27th February 2018, accepted 8th May 2018.*

Nowadays, extreme weather and rapid climate change are common topics discussed at all levels, i.e. scientifically, politically, and publicly (IPCC 2014). Comparisons with former climatic extremes are frequently employed in discussions aiming to address the stability/instability of regional environments and degree of environmental/human adaptation to climatic extremes at regional to global levels. The current study focuses on the interval between 24 and 22 cal. ka BP, which has been attested as one of the coldest and driest, although climatically unstable intervals of the late Quaternary (Lisiecki & Raymo 2005; Svensson *et al.* 2008).

The Baikal Region belongs to Siberia – a vast area of northern Eurasia with sparse human population, great variety of landscapes, extreme continental climate, the world's largest boreal forest belt, extensive permafrost (Alpat'ev *et al.* 1976), and a long history free from large continental ice sheets (Svendsen *et al.* 2004). This makes it an important region for palaeoenvironmental and earth system modelling studies (e.g. Kaplan *et al.* 2003; Melles *et al.* 2012; Schulz & Paul 2015), which provide a valuable contribution to the current knowledge on ecosystem development under extreme climate conditions

and facilitating future predictions and conservation strategies (Petit *et al.* 2008).

In recent decades, the palaeoenvironmental community working in different parts of Siberia has paid special attention to the coldest interval of the late Quaternary covering the time frame from *c.* 26.5 to 19 cal. ka BP (Clark *et al.* 2009) – the Last Glacial Maximum (LGM) – and its impact on the plant and animal communities (e.g. Guthrie 2001; Kienast *et al.* 2005; Willerslev *et al.* 2014), human populations (e.g. Dolukhanov *et al.* 2002; Fiedel & Kuzmin 2007), and regional climate, hydrology and geomorphology of the surrounding landscapes (e.g. Karabanov *et al.* 2004; Mangerud *et al.* 2008; Ganopolski *et al.* 2010; Kostrova *et al.* 2014). Despite significant progress in different study fields during recent years, the scarcity of high-resolution and well-dated LGM records remains a major obstacle for reliable environmental reconstructions in Siberia.

Müller *et al.* (2014) presented a detailed pollen record from Lake Kotokel in the Baikal region of Siberia (Fig. 1A), which covers the interval *c.* 27–19 cal. ka BP with an average temporal resolution of about 40 years. Their results suggest that cold steppe or/and herbaceous

tundra vegetation dominated in the study area through the entire analysed interval. In contrast to the relatively stable regional vegetation, the local environmental indicators, such as pollen of littoral plants and algae colonies, advocated for a greater sensitivity of the lake ecosystem to decadal- and century-scale climate variability (e.g. Shala *et al.* 2017). These findings encouraged researchers to continue investigating the remaining sediment using other proxies in an attempt to trace the climate variability in the study area.

In the current study, we present results of a multi-disciplinary study of Lake Kotokel sediments covering the interval 24–22 cal. ka BP. Newly obtained chironomid, ostracod, isotope, and geochemical records are discussed together with published environmental reconstructions derived from pollen and diatom records (Bezrukova *et al.* 2010; Kostrova *et al.* 2014; Müller *et al.* 2014) in order to explore the response of terrestrial vegetation and lake ecosystem to climate changes. In a final step, our results are compared with published LGM records from the

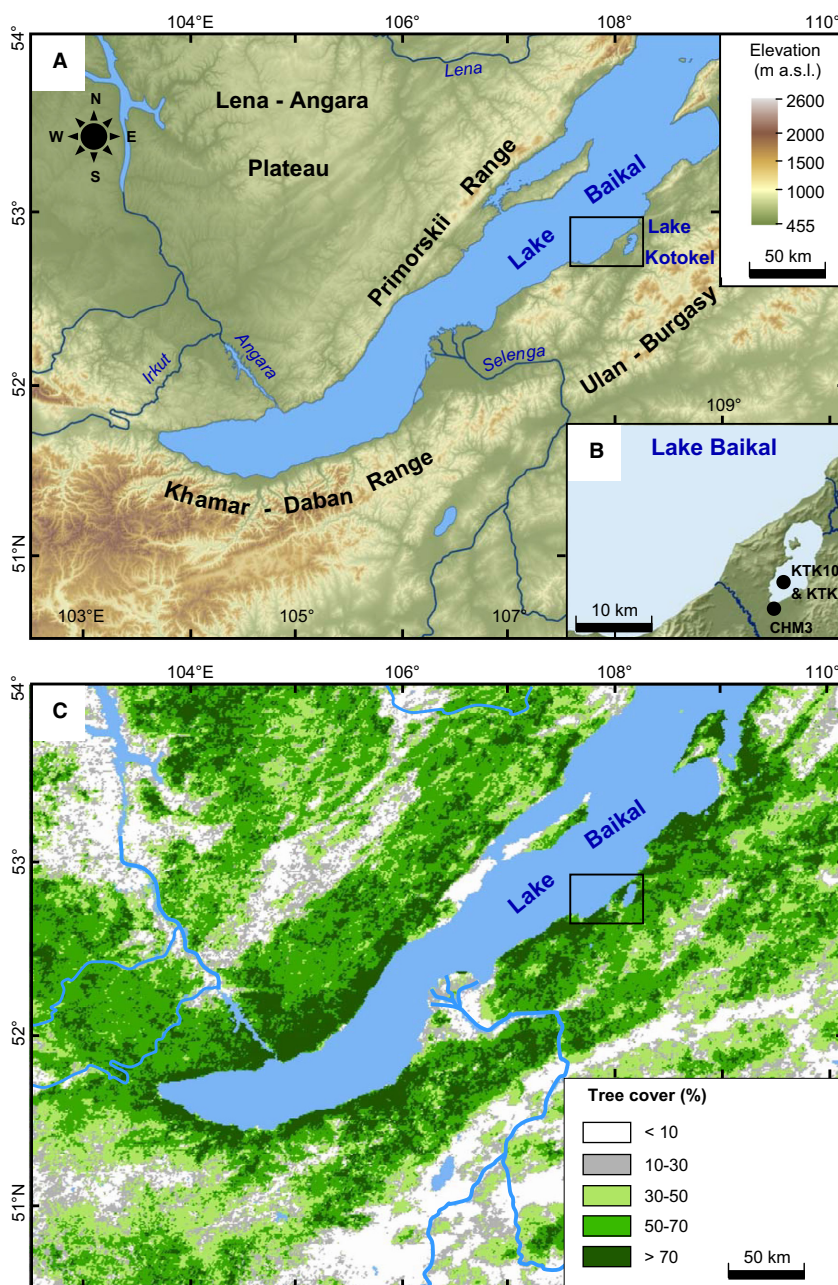


Fig. 1. A series of maps showing (A) the main topographic and hydrological features of the Lake Baikal region in southern Siberia, based on the Shuttle Radar Topography Mission (SRTM) v4.1 data (Jarvis *et al.* 2008), and location of the study area around Lake Kotokel (detailed in B); (B) the vicinity of Lake Kotokel and location of the sedimentary cores KTK2, KTK10, and CHM3 (black dots) discussed in the text; and (C) modern tree cover distribution based on the Advanced Very High Resolution Radiometer (AVHRR) dataset (DeFries *et al.* 2000).

Baikal region and more distant regions of the Northern Hemisphere.

### Lake setting and modern environments

Kotokel (latitude 52°47'N, longitude 108°07'E, altitude 458 m a.s.l.) is a freshwater lake situated 2 km east of Lake Baikal (Fig. 1B). The lake has an inflow from 15 to 20 streams and small rivers and an outflow to Lake Baikal (Kostrova *et al.* 2013). With a surface area of about 69 km<sup>2</sup> and a catchment area of about 187 km<sup>2</sup> (Zhang *et al.* 2013), it provides excellent conditions for pollen accumulation and preservation and for pollen-based reconstructions of local to regional vegetation and climate (Tarasov *et al.* 2009). A relatively short water residence time of about 7 years (Shichi *et al.* 2009) in association with a high abundance of diatoms, particularly in the Holocene sediment layers (Bezrukova *et al.* 2010; Fedotov *et al.* 2012), also makes Lake Kotokel sediments suitable for diatom analysis and diatom-based oxygen isotope studies (Kostrova *et al.* 2013, 2014). Pilot studies have also revealed the potential of the lake sediments for chironomid and ostracod analyses (Fedotov *et al.* 2012; Müller *et al.* 2014).

Lake Kotokel is located in a climatically sensitive biogeographical zone (Alpat'ev *et al.* 1976), which is comprised of species from boreal forest, steppe, and alpine tundra vegetation (Galaziy 1993). The climate is continental with long, cold winters and short, hot summers (Alpat'ev *et al.* 1976). The climate record from the nearby Cheremukhovo station documents a mean January temperature of −19.5 °C, mean July temperature of 15.4 °C, annual precipitation of about 400 mm, and 181 days with snow cover near the lake (Galaziy 1993). Almost half of the annual precipitation falls in July and August during increased southeastern cyclonic activity along the Mongolian branch of the Polar front, whereas between late autumn and early spring cold and sunny and generally dry weather associated with the stationary Siberian anticyclone predominates (Lydolph 1977; Kurita *et al.* 2004).

Modern vegetation along the eastern coast of Lake Baikal is mainly composed of boreal coniferous and deciduous forests (Fig. 1C) consisting of Scots pine, larch, and birch trees, with some admixture of aspen and shrubby alder (Galaziy 1993). Boreal evergreen conifers, including Siberian pine, fir, and spruce occupy the moist slopes of the Ulan-Burgasy Ridge, while alpine tundra communities with pine, alder and birch shrubs, grasses and sedges grow at altitudes above 1800 m (Molozhnikov 1986; Galaziy 1993). While tundra occupies large areas north and northeast of Lake Baikal, steppe vegetation is widespread on Baikal's largest island Olkhon and in the depressions along the Selenga River (Fig. 1C).

Bathymetric mapping and a geophysical survey performed in May 2011 (Zhang *et al.* 2013) revealed a maximal measured water depth of about 12 m in the northern part

between the island and the lake shore (Fig. 1B); however, the southern part of the lake, with an almost flat bottom, water depths of 3–4 m, and an up to 50-m-thick undisturbed sediment layer was suggested as the most promising for palaeoecological research. The first short sediment cores were recovered in this part of Lake Kotokel and results of coarse-resolution pollen and algal analysis were used for palaeoenvironmental interpretations (Korde 1968; Vipper 1968). Since then, several multi-disciplinary research teams have performed coring in the central part of the southern sub-basin and in Cheremushka Bog south of the lake reaching back to the LGM interval (e.g. Shichi *et al.* 2009; Bezrukova *et al.* 2010; Müller *et al.* 2014).

### Data and methods

#### *Analysed core material and revisited published records*

The Lake Kotokel sediments used for the environmental reconstructions and accompanying discussion in the current paper were obtained from the cores KTK2 (Bezrukova *et al.* 2010) and KTK10 (Müller *et al.* 2014) collected from the southern sub-basin (Fig. 1B) at a depth of about 3.5 m in August 2005 and July 2010, respectively. The coring sites are located about 1.8 km from the nearest shoreline and only a few metres apart from each other. A Livingston-type piston-corer of 7.5 cm diameter was applied to the upper and softer biogenic sediment and a 4.6-cm-diameter corer was used to penetrate the lower, more compact layers (Shichi *et al.* 2009; Müller *et al.* 2014). The focus interval 24–22 cal. ka BP in both cores consists of about 60 cm of dark-grey slightly laminated silty clay, with coarse-grained sand particles more abundant in the lower half of this unit (Müller *et al.* 2014). Remains of ostracods and chironomids were recognized in the LGM sediment, but not analysed in Müller *et al.* (2014).

The pollen analysis results and the age model based on 11 AMS radiocarbon measurements performed in the Poznan Radiocarbon Laboratory (Poland) allowed dating and robust correlation of the LGM sediment in the two cores (see Müller *et al.* 2014 for further details). The linear interpolation model (Müller *et al.* 2014) applied for the 2000-year interval discussed in the current study is supported by the two boundary radiocarbon dates 18 410 ± 100 <sup>14</sup>C a BP (Poz-40944) and 20 120 ± 90 <sup>14</sup>C a BP (Poz-52847). Their 95% confidence intervals obtained after calibration with the IntCal13 calibration curve (Reimer *et al.* 2013) using the OxCal v4.3 software package (Bronk Ramsey 1995) are 22 490–21 970 cal. a BP and 24 440–23 930 cal. a BP, respectively. The higher resolution analyses with an average temporal resolution of 30 to 60 years were all performed on the KTK10 core sediment.

In the current study, some of the previously published records were revisited and used in the re-analysis and/or in the discussion of the aquatic vs. terrestrial proxies. For

this purpose, we extracted results of the total inorganic carbon (TIC) and total organic carbon (TOC) determinations from the larger dataset representing the c. 27–19 cal. ka BP interval in the KTK10 core (Müller *et al.* 2014).

We also used results of pollen and non-pollen palynomorph (NPP) identification in the 62 samples from the KTK10 core record representing the 24–22 cal. ka BP interval discussed in the current study. These samples were microscopically analysed by Müller *et al.* (2014). We also refer to their work for the details of palynomorph extraction and identification and for the relevant references.

#### *Analysed proxies*

*Carbon and nitrogen determinations.* – Thirty-two samples – each representing 1-cm-thick sediment layer and taken in 2-cm steps – were analysed for carbon and nitrogen quantification. In the current work, we measured total nitrogen (TN) from the same samples that were analysed for TIC and TOC in Müller *et al.* (2014).

TN was analysed with a LECO Truspec Macro elemental analyser. For the detection of TC and TIC refer to Müller *et al.* (2014). Powdered samples of up to 200 mg were weighed into tin foil and the encapsulated sample was dropped into the primary furnace (950 °C) and flushed with pure oxygen for combustion. The sample aliquot gases were swept through hot copper (700 °C) to remove oxygen and change NO<sub>x</sub> to N, and Lecosorb (NaOH) and Anhydron (Mg(ClO<sub>4</sub>)<sub>2</sub>) to remove carbon dioxide and water. A thermal conductivity detector was used to determine nitrogen. Calibration standard soils (LECO 502-309; 1.05±0.03% nitrogen; LECO 502-308; 0.29±0.022% nitrogen) were used (RSD < 2%). The C/N ratio was calculated as the element mole ration of TOC (Müller *et al.* 2014) and TN.

*Ostracods.* – For the current study, ostracods were hand-picked from the KTK10 core sediment dated to 24–22 cal. ka BP. Ostracod shells were rarely intact, thus hampering precise taxonomic identification of specimens. Nevertheless, valves of *Cytherissa cf. lacustris* and the subfamily Candoninae were securely identified using a stereomicroscope and scanning electron microscope facilities at the FU Berlin (see Kossler (2010) for the methodological approach and references). The ostracod taxonomy is based on relevant species descriptions following the taxonomy in Meisch (2000). In the current work, the ostracod shells were used for stable isotope analyses, as described below.

*Chironomids.* – Sediment samples from the interval covering 24–22 cal. ka BP in the KTK10 core were analysed for head capsules of chironomids (non-biting midges). All available samples (each representing a 1-cm-thick layer of sediment accumulated during 30–35 years) were treated

for subfossil chironomid analysis following standard procedures outlined in Walker (2001) and Brooks *et al.* (2007). Sediments were deflocculated in 10% KOH at 75 °C for 10–15 min and washed through a 125-µm mesh sieve. Chironomid head capsules were picked out from the sieve residue in a Bogorov counting tray under a stereomicroscope at 20–40× magnification, dehydrated in 100% ethanol, and permanently mounted ventral side up on microscope slides using Euparal® as a mounting medium. As recommended by Heiri & Lotter (2001), at least 50 (mean = 82) chironomid head capsules were counted and identified in each sample in order to provide a representative count for quantitative analyses. Two samples (83.5 and 99.5 cm) are an exception, as they contained only 25–29 head capsules.

The chironomid remains were identified to genus or species-group morphotypes under a compound microscope at 200–400× magnification following identification keys by Brooks *et al.* (2007) and Andersen *et al.* (2013). Nomenclature of species-group morphotypes followed Brooks *et al.* (2007) with the exception for the genus *Propsilocerus*. The *Propsilocerus lacustris* species group represented by the two species *P. lacustris* and *P. paradoxus* with European and Asian distributions, respectively (Makarchenko & Makarchenko 2009), can be split easily into two species morphotypes within subfossil material using the descriptions in Sæther & Wang (1996) for both species, and Larocque-Tobler (2014) for European *P. lacustris* (described as *Propsilocerus*) from Polish lakes and Petrova *et al.* (2003) for Asian *P. paradoxus* from Lake Kenon in southern Siberia. The mentum of *Propsilocerus lacustris*-type has four median teeth subequal in size and the first lateral teeth are larger than the second ones (Larocque-Tobler 2014). In contrast, the *Propsilocerus paradoxus*-type mentum has a median portion with two to three small median teeth and one larger lateral pair and first lateral teeth that are distinctly shorter than the second ones (Petrova *et al.* 2003; Fig. 2).

*Ostracod-based δ<sup>18</sup>O and δ<sup>13</sup>C measurements.* – Two ostracod taxa were extracted from altogether 36 sediment samples and were prepared for stable oxygen isotope (δ<sup>18</sup>O) and stable carbon isotope (δ<sup>13</sup>C) analyses following the cleaning procedure described in Keatings *et al.* (2006). The stable isotope measurements of ostracod calcite were performed on a FINNIGAN MAT253 IRMS interfaced with an automated carbonate preparation device (KIEL IV) at the Deutsches GeoForschungsZentrum (GFZ) Potsdam. From each sample, about two valves of *Cytherissa cf. lacustris* or five of Candoninae (corresponding to 30–60 µg) were transferred into sample vials. In the KIEL IV device, samples were automatically dissolved with 103% H<sub>3</sub>PO<sub>4</sub> at 72 °C and the isotopic composition values were measured on the released and cryogenically purified CO<sub>2</sub>. The isotope ratios are expressed in delta per mil notation (δ, ‰) relative to VPDB and calibrated with IAEA standards NBS19 and NBS18. Replicated analysis



Fig. 2. Photomicrographs of larval menta of the chironomid *Propiloscerus paradoxus* from the Lake Kotokel sediment core: (A) the whole mentum and (B) the left lateral and median portions of the mentum.

of NBS19 yielded  $1\sigma$  standard deviations of  $0.04\text{‰}$  for  $\delta^{13}\text{C}$  and  $0.06\text{‰}$  for  $\delta^{18}\text{O}$ .

#### Quantitative approaches

**Numerical analyses.** – All numerical analyses presented in the current study were undertaken on pollen and chironomid taxa occurring in at least one sample with a relative abundance of more than 2%. Stratigraphical diagrams, showing the relative abundance of each taxon by sample depth and modelled age (cal. ka BP), were produced using TGView/Tilia (Grimm 2004) and C2 (Juggins 2007). To facilitate discussion of the stratigraphical record, the pollen and chironomid stratigraphies were subdivided into assemblage zones with the technique of optimal partitioning using sum-of-squares criteria (Birks & Gordon 1985) and the number of statistically significant zones was determined with the broken stick model (Bennett 1996), using the software package Psimpoll 4.27 (Bennett 2009). In order to summarize and estimate major trends in the pollen and chironomid assemblages through time, a detrended correspondence analysis (DCA) was applied to the biostratigraphical data to measure the gradient length of the first axis. The first DCA axis lengths were 0.6 and 2.3 SD units for the pollen and chironomid assemblages, respectively, suggesting that a linear response model and hence a principal components analysis (PCA) are appropriate for analysing both datasets. All ordinations were accomplished with the program CANOCO 5.0 (ter Braak & Šmilauer 2012) and statistically significant PCA axes were identified by comparison with a broken stick model (Bennett 1996) using the program BSTICK (J. M. Line and H. J. B. Birks, unpublished).

**Analysis of causal relationship between environmental variability and chironomid dynamics.** – The oxygen isotope records of diatoms from Lake Kotokel (Kostrova *et al.* 2014) indicate that the lake acted as a closed-basin hydrological system and effective moisture was one of the key factors controlling processes in the lake during the

last glacial. Taking into account that most relationships in nature are inherently nonlinear (e.g. Hilbert 2002; Burkett *et al.* 2005), nonlinear structural equation modelling (SEM; Grace 2006) employing classic (composite-based) and factor-based partial least squares (PLS) algorithms were used to explore multivariate causal relationships (paths) between the chironomid assemblage structure and water-level fluctuations, as a function of air temperature and effective moisture (precipitation minus evaporation). The SEM method differs from other modelling approaches as it tests the direct and indirect effects on pre-assumed causal relationships (Fan *et al.* 2016). The PLS algorithm is particularly useful when predictor variables are highly correlated (Wold *et al.* 2001). In order to test and separate the direct and indirect effects of water-level changes on the chironomid assemblages, the model fitted for the lake included three predictor latent variables (or drivers), ‘Water Level’, ‘Lake Productivity’, ‘Lake Sediments’, and the criterion latent variable (or response) ‘Chironomid Assemblages’. ‘Lake Productivity’ and ‘Lake Sediments’ were included as intermediate variables. The  $\delta^{18}\text{O}$  values of ostracods and the pollen-inferred annual precipitation were used as predictors (or indicators) of ‘Water Level’. The  $\delta^{13}\text{C}$  values of ostracods were used as a predictor (or an indicator) of ‘Lake Productivity’. All  $\delta^{18}\text{O}$  and  $\delta^{13}\text{C}$  values of *C. cf. lacustris* were corrected for Candoninae. The C/N ratio and TIC in the lake sediments were used as predictors (or indicators) of ‘Lake Sediments’. The relative abundances of chironomid taxa were included in the modelling as metrics (or indicators) of ‘Chironomid Assemblages’. The SEM analysis was implemented using the software package WarpPLS 5.0 and the Warp3 inner model algorithm (Kock 2015). As recommended by Kock (2015), the goodness of fit of the model with the data was assessed using average path coefficient (APC), average R-squared (ARS), average adjusted R-squared (AARS), and two quality indices: average block variance inflation factor (AVIF) and average full collinearity VIF (AFVIF). The statistical significance of path coefficients ( $\beta$ ) was estimated through jackknifing.

## Proxy records and interpretations

### Sediment geochemistry

The TIC, TOC, and TN values show only minor fluctuations throughout the investigated section. However, with respect to the TIC values and the C/N ratios two distinct zones, KTK-Gh-1 and KTK-Gh-2, have been identified (Fig. 3).

After *c.* 24 cal. ka BP (Zone KTK-Gh-1) the TIC shows values around the mean of 1.14% with highest values of up to 2% at *c.* 22.7 cal. ka BP. The TOC content varies between 2.0 and 4.1% (median 3.18%). The TN values parallel TOC and show values around 0.36% that are near the median of all analyses. Accordingly, the mean of the C/N ratio is 10 – but in peaks, ratios up to 13 are reached: three distinct peaks are observed at *c.* 23.7, *c.* 23.2 and *c.* 22.7 cal. ka BP.

After *c.* 22.5 cal. ka BP (Zone KTK-Gh-2) the TIC values decrease slightly and are below 1% (average 0.52%). TOC shows similar values as below and varies between 2.5 and 4.18%. The TN values show relatively constant values of around 0.4% and accordingly the C/N ratio is lower and averages around 9.5 without showing major changes.

Organic matter can be distinguished as originating from aquatic or land sources by its C/N ratio (Meyers & Ishiwatari 1995). The C/N ratio varies between 8 and 13, which are typical values for lacustrine sediments (Meyers & Teranes 2001). This suggests that the TOC mainly originates from lake algae, which commonly exhibit C/N ratios between 4 and 10, whereas vascular land plants (including aquatic macrophytes growing in the littoral zone) usually have C/N ratios of 20 and greater (Meyers

& Teranes 2001). The peaks in the C/N ratio may reflect a slightly increased contribution of aquatic macrophytes and/or terrestrial organic matter into the lake due to intensified erosion and/or higher water influx from in the catchment.

### Terrestrial pollen and NPPs

In the current study, 11 taxa (out of the 38 taxa identified by Müller *et al.* 2014) that exceed the 2% level in at least one sample were analysed using the broken-stick model. Based on this re-analysis the pollen record (Fig. 4) was partitioned into four statistically significant zones.

In the pollen assemblages of Zone KTK-Po-1 to Zone KTK-Po-4 (Fig. 4) herbaceous taxa absolutely predominate, whereas none of the tree/high shrub taxa exceed the 2% threshold, suggesting a virtually treeless LGM landscape. The most abundant pollen taxa are Poaceae, *Artemisia*, and Cyperaceae, followed by Asteraceae, Caryophyllaceae, and Ranunculaceae, all representative of steppe and herbaceous tundra vegetation in the Lake Baikal region (Bezrukova *et al.* 2010; Müller *et al.* 2014).

The pollen assemblages of Zone KTK-Po-1 (*c.* 24.0–23.7 cal. ka BP) and Zone KTK-Po-3 (*c.* 23.3–22.4 cal. ka BP) reveal the relatively low percentages of Ranunculaceae and the relatively high contributions of *Artemisia*. A pronounced feature of Zone KTK-Po-2 (*c.* 23.7–23.3 cal. ka BP) is a threefold increase in the proportion of Ranunculaceae (buttercup or crowfoot family) pollen. A second, although less pronounced peak of Ranunculaceae appears in Zone KTK-Po-4 (*c.* 22.4–22.0 cal. ka BP) and is accompanied by the lowest content of *Artemisia* pollen, almost complete disappearance of Brassicaceae, the highest proportions of Caryophyllaceae and Asteraceae, and relatively high percentages of Poaceae and Cyperaceae. The Ranunculaceae pollen probably represent littoral/meadow vegetation. A number of interpretations involving various representatives of the Ranunculaceae family native to marshes, fens, and wetlands and flourishing in a landscape inundated with snow-melt waters (e.g. regional native *Caltha palustris* and *Ranunculus reptans*) can be suggested (Müller *et al.* 2014). Littoral pioneer vegetation communities with Ranunculaceae species occupy erosive soils in the range of fluctuating water levels at shores of shallow lakes and regularly inundated depressions (Hilbig 1995; Dierßen & Dierßen 1996). The plant macrofossil record (Kienast *et al.* 2005) suggests they were a characteristic component of the LGM vegetation mosaic in eastern Siberia.

The PCA ordination applied to the pollen record produces two statistically significant axes (Fig. 4). These two axes together explain 71% of the total variance in the pollen assemblages. The first axis clearly separates Zone KTK-Po-4 (*c.* 22.4–22.0 cal. ka BP), characterized by the low abundance of dryness-adapted *Artemisia*, from all other samples. Such a distribution of the assemblages along PCA axis 1 suggests that this axis can be interpreted

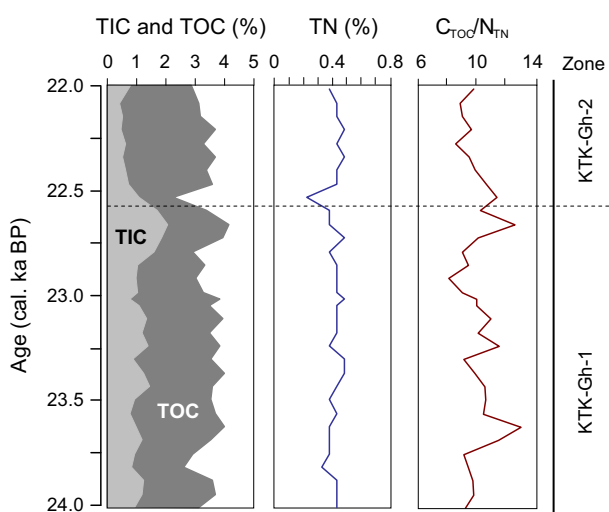


Fig. 3. Geochemistry of the KTK10 core sediment dated to 24–22 cal. ka BP: total organic carbon (TOC), total inorganic carbon (TIC), total nitrogen (TN) percentage values, and C/N ratio are shown.

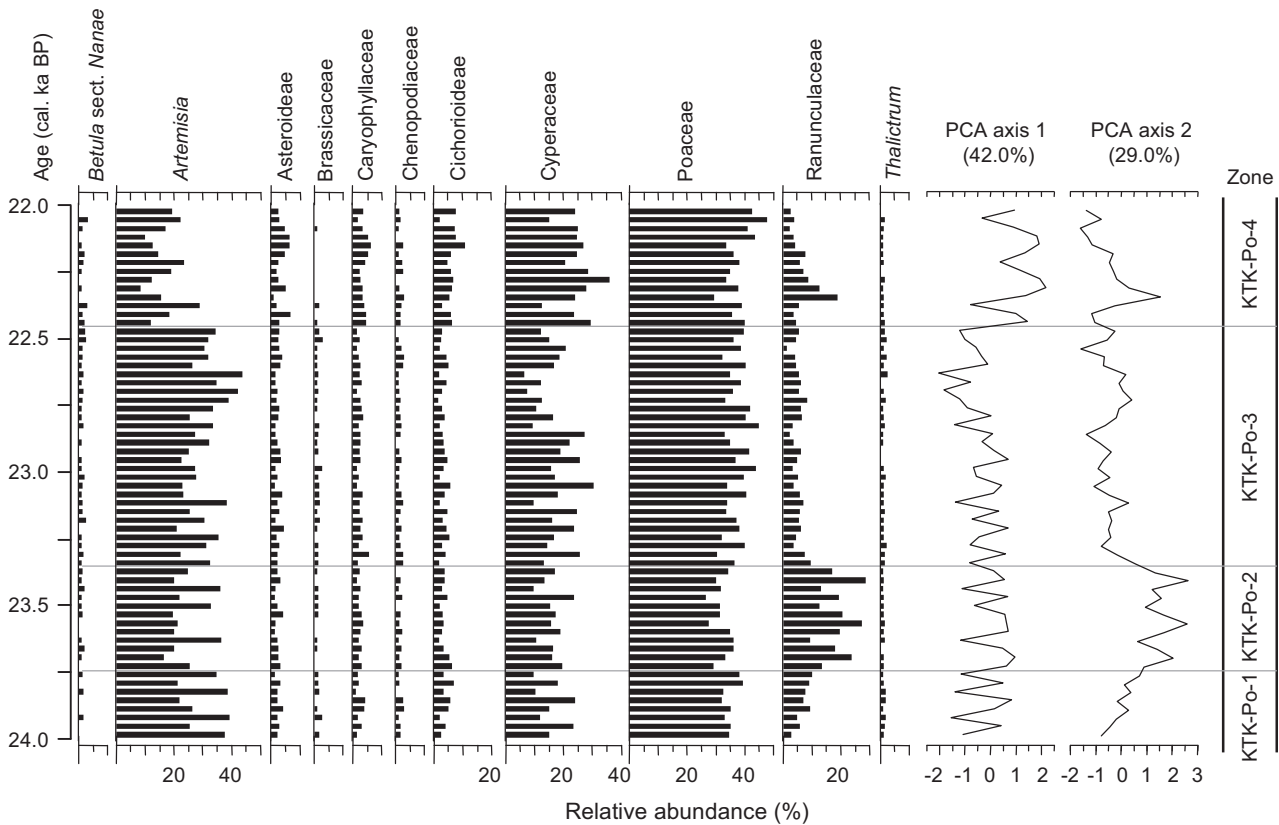


Fig. 4. Relative abundances of selected pollen types, sample scores of the first two PCA axes, and statistically significant zones (this study) for the pollen stratigraphy in the KTK10 sediment core dated to 24–22 cal. ka BP. Taxa percentages refer to the total sum of terrestrial pollen grains.

to mainly reflect an atmospheric precipitation gradient in the study area. The weaker second axis is driven largely by the proportion of Ranunculaceae, reflecting an extension of shallow-water and wet meadow biotopes.

The NPP diagram (Fig. 5) shows three most representative taxa with percentages exceeding the 2% level in more than one sample. The *Pediastrum* curve demonstrates four distinct minima (40–45%) and four maxima (75–85%) during the study interval. Green algae representing this genus are often found in freshwater bodies, mostly shallow and rich in organic matter. Therefore, *Pediastrum* fluctuations may indicate changing water depth, with a deepest phase occurring after *c.* 22.5 cal. ka BP, in line with the lowest contents of *Artemisia* pollen. Prior to this date, the *Pediastrum* percentages are in good correspondence with the changes in the C/N ratio (Fig. 3), supporting our interpretation. Relatively low proportions of *Botryococcus* and *Glomus* spores are recorded between *c.* 24.0 and 22.6 cal. ka BP. A distinct increase in the proportion of *Glomus* (up to 5–10%) at *c.* 22.4–22.0 cal. ka BP corresponds well with the uppermost pollen zone, which reveals the second peak in Ranunculaceae. Spores of this fungus, which occurs in a variety of host plants, including a number of herbaceous plant families, are reported to be especially abundant in late glacial environments with highly eroded soils (Demske *et al.* 2016).

#### *Ostracods and ostracod-based isotope records*

Valves of *Cytherissa cf. lacustris* and the subfamily Candoninae show almost continuous presence throughout the analysed interval (Fig. 6). Candoninae is present in the lower part of the record and disappears at *c.* 22.4 cal. ka BP. An interval between *c.* 22.6 and 22.4 cal. ka BP reveals an overlapping occurrence of Candoninae and *C. cf. lacustris*. The latter taxon alone represents the uppermost part of the record.

*Cytherissa lacustris* is a benthic ostracod with a parthenogenetic mode of reproduction and Holarctic distribution. The ecological field studies characterize this species as being restricted to oligotrophic lakes where water temperatures do not exceed 18 °C. Nevertheless, in laboratory experiments the temperature limit of this taxon was found to be wider, up to 20 °C (see Newrkla (1985) for a summary and references). Palaeolimnological studies in alpine lakes showed that the onset of eutrophication, and coupled changes in the sediment structure, which make locomotion difficult (Powell 1976), coincide with the disappearance of *C. lacustris* (Löffler 1969). In order to avoid these unsuitable conditions, amongst others decreasing oxygen supply, the ostracods have to migrate to the littoral zone, where they are restricted to temperatures below 18–20 °C (Löffler 1971). *Candona candida*

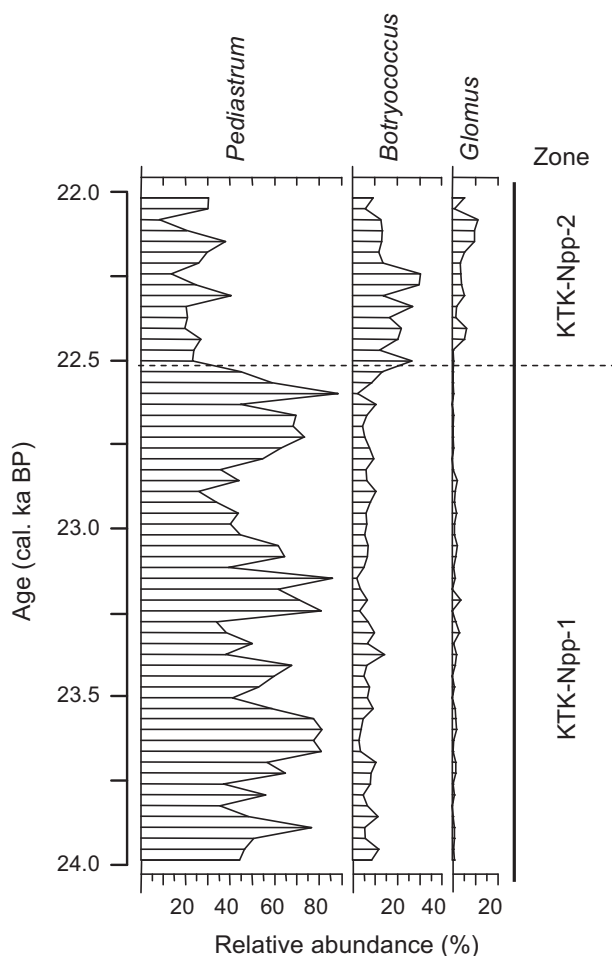


Fig. 5. Selected results of the non-pollen palynomorph (NPP) analysis of the KTK10 core sediment dated to 24–22 cal. ka BP. Taxa percentages refer to the total terrestrial pollen sum plus the sum of palynomorphs in the respective NPP group (following Müller *et al.* 2014).

and *C. lacustris* are abundant taxa in the extreme continental climate of Yakutia, where they tolerate significant variations in salinity and temperature (Kienast *et al.* 2011). Study of the ostracod assemblage at Attersee, Austria, demonstrated that *Candona* sp. outnumbers *C. lacustris* in the littoral shallower zone, whereas *C. lacustris* is at its maximum density at higher depths with a temperature range of 5–15 °C (Newrkla 1985). Substitution of *Candona* by *C. cf. lacustris* in the KTK10 core sediment could, therefore, reflect an increase in water depth after *c.* 22.6 cal. ka BP.

The results of the stable isotope analyses show that the  $\delta^{13}\text{C}$  values range between  $-4$  and  $+4\text{‰}$  and the  $\delta^{18}\text{O}$  values between  $-11$  and  $-4\text{‰}$  for both *Candona* and *C. cf. lacustris* from *c.* 24 to 22 cal. ka BP (Fig. 6). In general, carbon isotopes in ostracod calcite are in equilibrium with dissolved inorganic carbon (DIC) contents (von Grafenstein *et al.* 1999) and reflect water temperature, pH and productivity in the habitat of different species (Decrouy *et al.* 2011). The stable isotope  $\delta^{13}\text{C}$  values of

*Candona* range from  $+0.6$  to  $+4\text{‰}$ , while *C. cf. lacustris* shows lighter values varying between  $-4$  and  $0\text{‰}$ . The difference between the mean values of the two taxa is about  $4\text{‰}$ . *Candona* shells with  $\delta^{13}\text{C}$  values of about  $+4\text{‰}$  indicate depletion in  $^{12}\text{C}$  and consequently enriched DIC, inducing eutrophication and leading to enhanced phytoplankton biomass and primary production, and increased turbidity. The lighter  $\delta^{13}\text{C}$  values of *C. cf. lacustris* may indicate individuals that occupied deeper water habitats, with high bioavailability of lighter carbon released from decomposing organic matter.

The  $\delta^{18}\text{O}$  value of lake carbonates is mainly influenced by the oxygen isotopic composition of precipitation and river runoff, temperature, and evaporation. In hydrologically closed lakes  $\delta^{13}\text{C}$  and  $\delta^{18}\text{O}$  values often co-vary due to evaporation (Leng & Marshall 2004). Today, Lake Kotokel is an open lake system, but the oxygen isotopes in carbonate shells from the KTK10 record mainly seem to be affected by evaporation and suggest that the lake acted as a closed-basin hydrological system under relatively dry and cool conditions between *c.* 24 and 22 cal. ka BP. In the lower part of the record, *Candona* valves are characterized by heavier mean  $\delta^{18}\text{O}$  values of  $-6.1\text{‰}$  before *c.* 23.2 cal. ka BP, while they show lighter  $\delta^{18}\text{O}$  values of about  $-8.6\text{‰}$  in the upper part, after *c.* 22.9 cal. ka BP, equal to a shift of  $+2.5\text{‰}$ . *Candona* disappear at *c.* 22.4 cal. ka BP, but their overlapping occurrence with *C. cf. lacustris* between *c.* 22.6 and 22.4 cal. ka BP reflects the similarity of the  $\delta^{18}\text{O}$  values of these two taxa. During this time-span, the mean  $\delta^{18}\text{O}$  values are  $-8.9$  and  $-10.1\text{‰}$  for *Candona* and *C. cf. lacustris*, respectively, and the difference between these taxa corresponds to the ‘vital effect’ of about  $1\text{‰}$  inferred by von Grafenstein *et al.* (1999).

Ostracods from the lowest part of the record show significantly heavier  $\delta^{18}\text{O}_{\text{mean}}$  values of around  $-6\text{‰}$  with high variation (ranging between  $-8.6$  and  $-3.8\text{‰}$ ), suggesting enhanced evaporation and lake-level changes due to cooler and dryer conditions from *c.* 24.0 to 23.2 cal. ka BP. Comparison with the GISP2 potassium ion record (Mayewski *et al.* 1997) indicates a very strong Siberian high during this time. Evidence for substantially cooler than present conditions in the Northern Hemisphere was also found in the NGRIP  $\delta^{18}\text{O}$  record (Svensson *et al.* 2008). The lighter oxygen isotope values ( $\delta^{18}\text{O}_{\text{mean}} = -8.6\text{‰}$ ) of both taxa from the upper part of the KTK10 record, lower  $\text{K}^+$  contents in the GISP ice-core, and heavier  $\delta^{18}\text{O}$  values in the NGRIP ice-core coincide with lower evaporation, a weaker Siberian high, and warmer than before conditions after *c.* 23.2 cal. ka BP.

#### *Chironomids and causal relationship with environmental variability*

In total, 13 chironomid taxa were identified in the analysed sediment samples and eight of these have abundances  $>2\%$  in at least one sample (Fig. 7). Rare taxa (abundance  $<2\%$ )

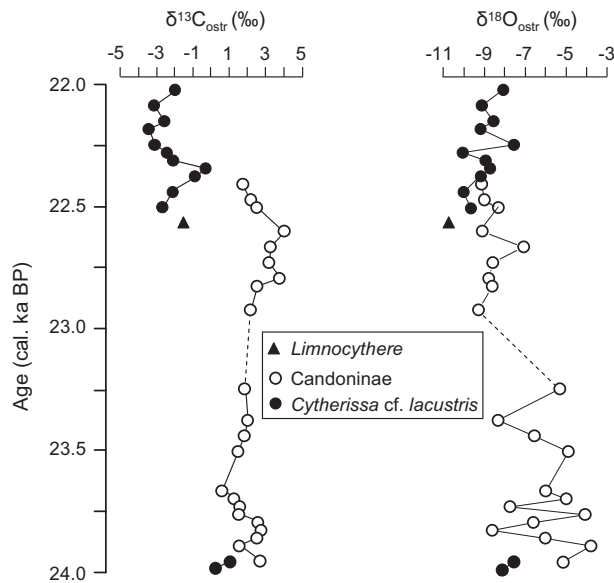


Fig. 6. Distribution of the ostracod taxa identified in the KTK10 core sediment dated to 24–22 cal. ka BP and results of the isotopic analyses performed on the recovered shells.

are *Constempellina-Thienemanniola*, *Corynocera ambigua*-type, *Glyptotendipes*, and *Polypedilum nubifer*-type. The chironomid record was partitioned into three statistically significant zones (Fig. 7).

Zone KTK-Ch-1 (c. 24.0–23.4 cal. ka BP) is dominated by *Chironomus anthracinus*-type (50–100%), which is usually associated with relatively shallow-water habitats of lakes (Nazarova *et al.* 2011; Luoto 2012). The relative abundances of *Sergentia coracina*-type, which prefers deep-water habitats of cold lakes (Pankratova 1983), do not exceed 4%. Most likely, a low lake stand due to decreased effective moisture induced by relatively cool and dry climatic conditions occurred during this period.

Zone KTK-Ch-2 (c. 23.4–22.5 cal. ka BP) reveals relatively high values of *Chironomus anthracinus*-type (between 35 and 88%), although a decrease down to 25% occurs within the upper part of the zone. At the beginning of this zone, the typical deep-water inhabitant *Tanytarsus lugens*-type (Hofmann 1988; Nazarova *et al.* 2011) appears and becomes co-dominant (up to 58%) with *C. anthracinus*-type. The chironomid *S. coracina*-type is present sporadically (up to 8%) through the lower and middle parts of the zone. *Microtendipes pedellus*-type, a taxon that is commonly associated with littoral habitats and indicative of moderate to warm temperatures (Brodersen & Lindegaard 1997), appears for the first time in the record at abundances of 2–6%. A sudden increase in *T. lugens*-type suggests a rapid lake-level rise as a result of a climatic shift towards wetter conditions at the beginning of this period. Under a warming climate, enhanced lake productivity may have strengthened the oxygen consumption in the sediments. This interpretation is supported by the sporadic appearances of the

sediment-dwelling, deep-water inhabitant *Prosilocerus paradoxus* that is, as well as other *Prosilocerus* species, a good indicator of hypertrophic conditions in lakes (Petrova *et al.* 2003; Kornijów & Halkiewicz 2007).

Zone KTK-Ch-3 (c. 22.5–22.0 cal. ka BP) displays a strong change in assemblages: a distinct increase in *P. paradoxus*-type (up to 40%) and *Procladius* (up to 12%), dominance of *T. lugens*-type (49–75%), as well as the disappearance of *C. anthracinus*-type. The high abundance of *P. paradoxus*-type, an indicator of hypertrophic conditions, together with the presence of *Procladius*, a taxon indicative of high lake productivity (Brodersen & Quinlan 2006) and tolerant of low oxygen levels (Brodersen *et al.* 2004), may suggest an increase in lake productivity and sediment oxygen depletion following organic enrichment. The dominance of *T. lugens*-type, a taxon living on the sediment surface and intolerant of low oxygen levels, suggests that the concentrations of dissolved oxygen in the water remain high during most of the year. Most likely, this period corresponds to the onset of relatively warmer and wetter conditions, when the rate of precipitation exceeded the rate of evaporation, resulting in increased effective moisture and a relatively highstand of the lake. Unfortunately, *P. paradoxus*-type is not present in any of the existing chironomid–climate calibration datasets. However, a detailed analysis of the *P. paradoxus* life cycle in another lake of the Baikal region (i.e. Lake Kenon; 360 km southeast of Lake Kotokel) has provided evidence that the emergence of the adults begins when the bottom water temperature reaches 13–16 °C, and the hatching of larvae from eggs starts when the water temperature reaches 19–21 °C (Petrova *et al.* 2003). Therefore, most likely, the lake remained unstratified and bottom water temperatures reached at least 19 °C in summer.

The PCA ordination applied to the chironomid stratigraphy produces only one statistically significant axis that explains more than 82% of the total variance in the chironomid data (Fig. 7). Taking into account the habitat preferences of chironomid taxa and the structural changes in the assemblages along the first PCA axis, this axis is interpreted to mainly reflect a water-level gradient. Over time, the PCA1 scores shifted to positive values, indicating a lake-level rise, which was associated with the replacement of *C. anthracinus*-type by *T. lugens*-type and *P. paradoxus*-type.

The results of the SEM analysis showed that 53% of the variance in the chironomid assemblages of Lake Kotokel can be explained by the predictor variables, such as Water Level, Lake Productivity, and Lake Sediments (Fig. 8). The pathway between Water Level and Lake Productivity was much stronger ( $\beta = -0.51$ ,  $p < 0.01$ ) than those between Water Level and Lake Sediments ( $\beta = 0.29$ ,  $p < 0.01$ ) or between Water Level and Chironomid Assemblages ( $\beta = -0.24$ ,  $p < 0.01$ ). The pathway between Lake Sediments and Chironomid Assemblages was stronger ( $\beta = -0.42$ ,  $p < 0.01$ ) than those between Lake Productivity and Chironomid

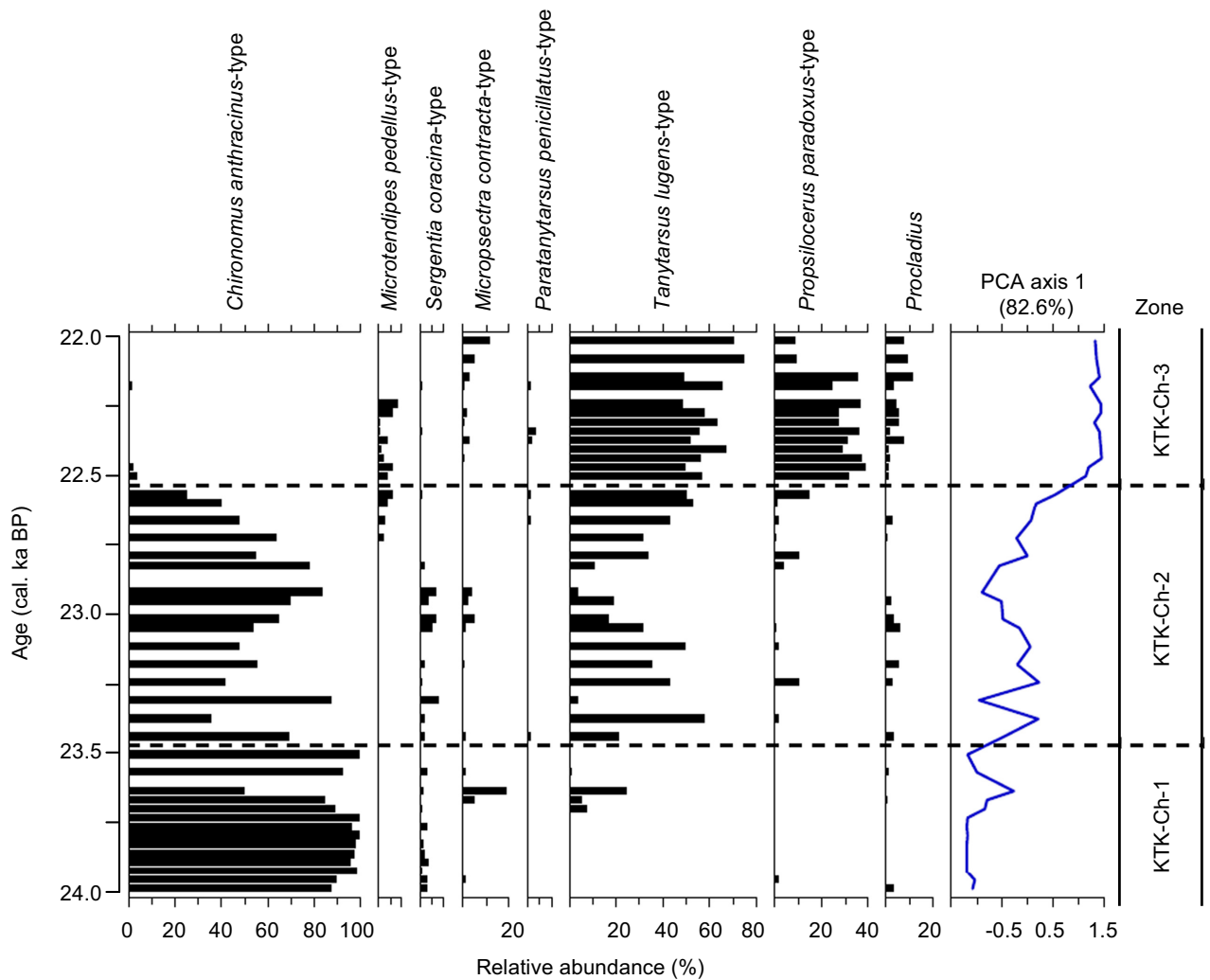


Fig. 7. Relative abundances of selected chironomid taxa, sample scores of the first PCA axis, and statistically significant zones for the chironomid stratigraphy in the KTK10 sediment core dated to 24–22 cal. ka BP.

Assemblages ( $\beta = 0.32$ ,  $p < 0.01$ ) or between Lake Productivity and Lake Sediments ( $\beta = -0.32$ ,  $p < 0.01$ ). The results suggest that lake-level changes, as a function of air temperature and effective moisture, were the factor that most strongly and directly affected pelagic productivity of the lake. The direct effects of lake-level changes on the chironomid assemblages were weaker than their indirect effects mediated through processes impacting the lake pelagic productivity and sediment characteristics. These findings agree with those of Hofmann (1998), who suggested that water-level changes produce weak direct effects on invertebrate assemblages.

## Discussion

### *The aquatic vs. terrestrial proxy records of the LGM environments from Lake Kotokel*

In this section, newly obtained chironomid, ostracod, isotope, and geochemical records derived from the mul-

tidecadal sedimentary archive of Lake Kotokel are used in concert with the published environmental reconstructions in order to explore the terrestrial vegetation and lake ecosystem responses to climate changes during the time interval 24–22 cal. ka BP.

The interpretations based on the published results of pollen analyses (Shichi *et al.* 2009; Bezrukova *et al.* 2010; Müller *et al.* 2014) suggest that herbaceous vegetation dominated in the study area around Lake Kotokel through the entire analysed interval. This qualitative interpretation is supported by quantitative vegetation reconstructions using the pollen-based method of ‘biomization’ (Prentice *et al.* 1996). Indeed, the ‘biomization’ approach applied to the KTK2 (Bezrukova *et al.* 2010) and KTK10 (Müller *et al.* 2014) pollen records demonstrates that the cold steppe biome had the highest scores, followed by the tundra biome (Fig. 9A). The minor fluctuations in the calculated biome scores were interpreted as evidence of general stability of the regional vegetation cover during the LGM (Müller *et al.* 2014). This interpretation, however,

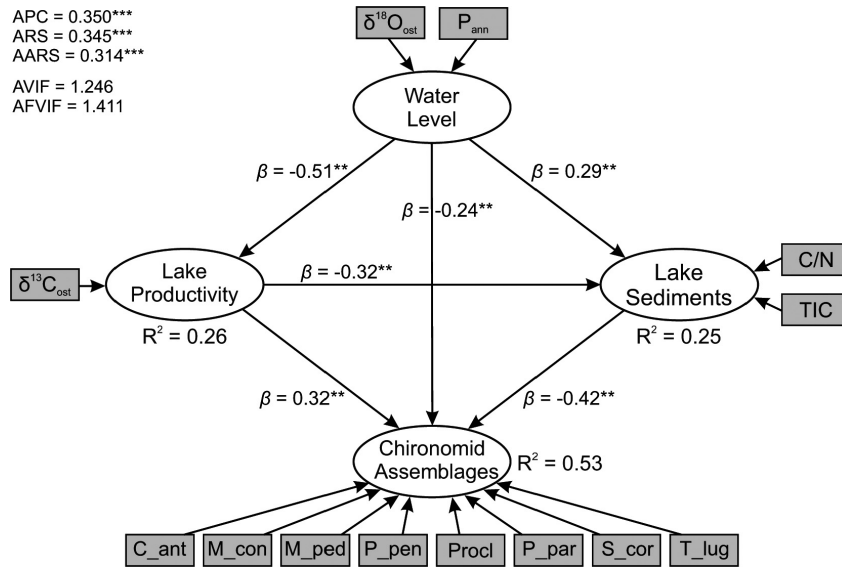


Fig. 8. The structural equation model used to explore the direct and indirect effects of lake-level fluctuations on the chironomid assemblages in Lake Kotokel. The strength of the causal influence of each path is denoted by the path coefficient ( $\beta$ ) adjacent to the respective arrow. Observed variables: pollen-inferred annual precipitation ( $P_{\text{ann}}$ ), stable carbon and oxygen isotope values of ostracods ( $\delta^{13}\text{C}_{\text{ost}}$  and  $\delta^{18}\text{O}_{\text{ost}}$ ), the C/N ratio and total inorganic carbon (TIC) content in the lake sediment, and the relative abundances of chironomid taxa: C\_ant = *Chironomus anthracinus*-type; M\_con = *Micropsectra contracta*-type; M\_ped = *Microtendipes pedellus*-type; P\_pen = *Paratanytarsus penicillatus*-type; Procl = *Procladius*, P\_par = *Propilocerus paradoxus*-type; S\_cor = *Sergentia coracina*-type; T\_lug = *Tanytarsus lugens*-type. Asterisks indicate level of statistical significance:  $^{**}p < 0.01$ ,  $^{***}p < 0.001$ . The model fit and quality indices: average path coefficient (APC), average R-squared (ARS), average adjusted R-squared (AARS), average block variance inflation factor (AVIF) and average full collinearity VIF (AFVIF).

does not resolve the question of whether the reconstructed vegetation cover stability is a function of stable LGM climate or if it can be explained by a greater tolerance of herbaceous plants and biomes to LGM climate fluctuations. Modelling experiments suggest that both cold steppe and herbaceous tundra can tolerate a wide range of temperatures under relatively dry arctic to boreal climates (Kaplan *et al.* 2003), thus indicating a need to search for other, more sensitive indicators. Variable contents of semi-aquatic/wet meadow plant (i.e. Ranunculaceae) pollen and green algae (i.e. *Pediastrum*) colonies in the KTK10 core (Figs 4, 5; Müller *et al.* 2014) also advocate for a greater sensitivity of the lake ecosystem to shorter-term climate variability.

In earlier studies, the peaks in Ranunculaceae were interpreted in terms of a much shorter than present distance between the KTK10 coring site and the palaeo-shoreline, reflecting a smaller area of the lake and the generally drier-than-present LGM climate (Zhang *et al.* 2013; Müller *et al.* 2014). Another proposed interpretation involved short-term episodes with higher soil erosion (Müller *et al.* 2014). This hypothesis mainly relies on the increase in coarse-grained sand particles that parallels the high Ranunculaceae pollen percentages at *c.* 23.7–23.3 cal. ka BP. The relatively high percentages of *Glomus* at *c.* 22.4–22.0 cal. ka BP (Fig. 5) might also point to intensified soil erosion (Müller *et al.* 2014).

A third scenario is proposed here, which can be tested with the newly obtained ostracod and chi-

ronomid data. This scenario implies that the peaks in Ranunculaceae pollen point to periods of substantial lake-level fluctuations. As a rule, fluctuating water levels increase the area of shoreline wetlands, whereas any stabilization of water levels reduces this area (Keddy & Reznicek 1986; Mortsch 1998). The relative abundance of Ranunculaceae pollen, representing near-shore semi-aquatic/wet habitats, may therefore reflect the wetland ecosystem responses to lake-level fluctuations. The first short-term appearance of deeper-water *T. lugens*-type in the chironomid record around 23.7 cal. ka BP (Fig. 7) and a distinct peak in the C/N ratio (Fig. 3) coincide with the first peak in Ranunculaceae pollen (Fig. 4), supporting the latter interpretation. In addition, the Ranunculaceae record (and pollen PCA axis 1), as well as the chironomid PCA axis 1, suggests substantial water-level fluctuations between *c.* 23.7 and 23.3 cal. ka BP. These fluctuations could be one of the main reasons for higher soil erosion and the increase in coarse-grained sand particles through this time interval. Both the  $\delta^{18}\text{O}$  ostracod record (Fig. 6) and pollen-based precipitation reconstruction (Fig. 9B; Tarasov *et al.* 2017) suggest a relatively shallow lake and relatively dry climate, which however do not exclude short-term lake level fluctuations and associated lakeward and landward shifts in wetland habitats. During the second peak in Ranunculaceae around 22.3 cal. ka BP, all proxies point to a slightly deeper

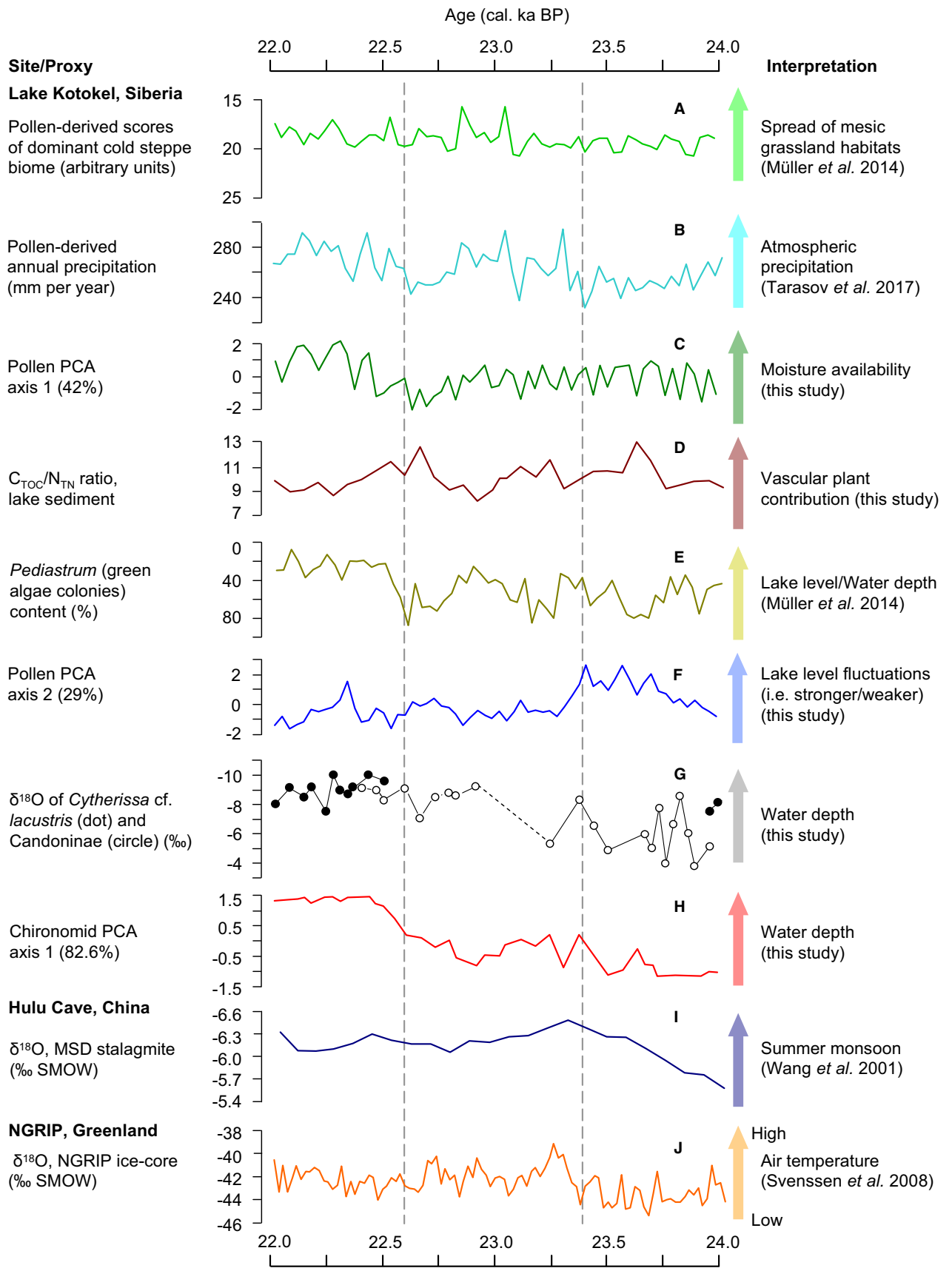


Fig. 9. Summarized records of the terrestrial and aquatic proxies from the Lake Kotokel sediment discussed in this study (A–H) along with the selected proxies representing regional and hemispheric records of climate variability during the interval in focus. (A) and (E) are modified from Müller *et al.* (2014); (B) – from Tarasov *et al.* (2017); (C), (D), and (F–H) – from this study; (I) – from Wang *et al.* (2001); and (J) – from Svensson *et al.* (2008). Note: to facilitate a direct comparison, values along the vertical axis in (A), (E), (G), and (I) are plotted in reversed order. Vertical dashed lines signify the three main phases in Lake Kotokel's development: the driest phase (*c.* 24.0–23.4 cal. ka BP) with low precipitation, high summer evaporation, and low lake levels; the transitional phase (*c.* 23.4–22.6 cal. ka BP); and the phase (*c.* 22.6–22.0 cal. ka BP) of relatively high precipitation (and moisture availability) and relatively deep lake.

than before Lake Kotokel and slightly higher, although variable, atmospheric precipitation, which could explain the rapid changes in the lake level.

All three scenarios generally agree on a smaller-than-present size of the lake and proximity of the coring site to the lake shore during the whole study period, as suggested by a study on the basin morphology and seismic stratigraphy of Lake Kotokel (Zhang *et al.* 2013). The latter interpretation is also supported by the dominance of the small benthic and virtual absence of planktonic diatoms during the interval *c.* 24–22 cal. ka BP (Bezrukova *et al.* 2010). The pollen assemblage composition, however, points to generally moister environments during the interval with the lowest *Artemisia* percentages (*c.* 22.4–22.0 cal. ka BP).

A major drop in *Pediastrum* accompanied by a twofold increase in *Botryococcus* percentages pre-dates the KTK-Po-3/KTK-Po-4 pollen zone boundary by about 50 years, suggesting that the lake ecosystem was either more sensitive or reacted faster to climate change than terrestrial steppe vegetation in the region. The second interpretation is more likely, regarding a low sensitivity of the cool grass/shrub plant functional type and non-forest biomes (Prentice *et al.* 1996) to the temperature changes (Kaplan *et al.* 2003). Alternatively, high-resolution pollen and diatom studies on the late glacial sediment from Lake Suigetsu, central Japan (Kossler *et al.* 2011) demonstrated a rapid response of the entire lacustrine and terrestrial system to climate changes. Despite the fact that the diatom and sediment records of Lake Suigetsu showed more abrupt shifts from warm to cold (and cold to warm) environments than the temperature-sensitive temperate deciduous forest biome (Prentice *et al.* 1996), the authors did not find any delayed response of local vegetation to climate change (Kossler *et al.* 2011).

The mentioned changes in the NPP record of Lake Kotokel are accompanied by a distinct minimum in the TIC, TOC and TN percentages around 22.5 cal. ka BP (Fig. 3). Nevertheless, the observed trend towards the lowest values starts some decades earlier and parallels a decrease in *Artemisia* pollen percentages (Fig. 4) representing changes in the upland vegetation. Comparable trends can be seen in the ostracod (Fig. 6) and chironomid (Fig. 7) records, in which distinct compositional shifts occurred between *c.* 22.6 and 22.5 cal. ka BP. These results corroborate the previous study on Lake Suigetsu showing that pollen-derived disturbances in the forest vegetation reflect regional cooling and warming shifts that started at least two to three decades prior to the major change in the

inorganic lake sediment (e.g. appearance/disappearance of detrital layers) and in diatom assemblages (Kossler *et al.* 2011).

The diatom analysis of the KTK2 core sediment demonstrated extremely poor preservation or total absence of diatoms during the LGM interval (Bezrukova *et al.* 2010), thus preventing the use of this otherwise informative proxy for the reconstruction of palaeoenvironments. The coarse-resolution diatom record available shows a dominance of small valves of the *Staurosirella pinnata* agg. complex between *c.* 24 and 22 cal. ka BP (Bezrukova *et al.* 2010). The tychoplanktonic *Staurosirella pinnata* can be abundant in relatively warm, shallow, eutrophic lakes with high pH (Bennion 1994), although it is more widely known for developing large populations in arctic and alpine lakes under cold and oligotrophic conditions (Lotter *et al.* 2010; Li *et al.* 2015). It is considered an opportunist taxon that takes advantage of repeated disturbances (Lotter & Bigler 2000) in line with the interpretation in Bezrukova *et al.* (2010) and with the records of lake-level fluctuations presented in the current study. The very low diatom concentrations in the LGM sediment of Lake Kotokel also hindered their extraction and purification for isotope analysis (Kostrova *et al.* 2014). The results obtained for the four samples of the KTK2 core from the *c.* 24–23 cal. ka BP interval display relatively high  $\delta^{18}\text{O}$  diatom values of about 30.1‰ prior to 23.3 cal. ka BP, interpreted as a combined effect of low atmospheric precipitation and relatively high evaporation during the summer time (Kostrova *et al.* 2014). The latter study also reported a noticeable spike of 28.7‰ at about 23.2 cal. ka BP that is broadly synchronous with an oscillation in the NGRIP  $\delta^{18}\text{O}$  record (Fig. 9F; Svensson *et al.* 2008) and in the KTK10 isotope record of ostracods presented here (Fig. 9G), that may reflect an additional water input as a reaction to hemispheric temperature increase (Kostrova *et al.* 2014).

The analysed key proxies from the Lake Kotokel sedimentary archive representing terrestrial and aquatic environments during the selected interval are summarized in Fig. 9A–H. Upland vegetation dynamics are mirrored in the scores of the cold steppe biome (Fig. 9A) that absolutely dominate in the regional vegetation cover. Except for a minor gradual trend towards lower values suggesting a turn to slightly wetter climate conditions after *c.* 23.4 cal. ka BP, the biome scores remain relatively stable, which probably indicates overall stability of the vegetation cover. The pollen-derived atmospheric precipitation (Fig. 9B) corroborates the main trend in

vegetation development, although the reconstructed shift to higher values and greater fluctuations after *c.* 23.4 cal. ka BP is more obvious in this case. The pollen PCA axis 1 (Fig. 9C) explains 42% of the variation, suggesting a strong response of the pollen composition to changes in the regional vegetation and associated climate. The most pronounced feature in this curve is the interval with highest values, representing a phase with less arid vegetation and climate between *c.* 22.6 and 22.0 cal. ka BP. The observed differences in the curves in Fig. 9A–C may indicate that the pollen PCA axis 1 represents changes in the regional moisture availability (i.e. ‘moisture index’ *sensu* Prentice *et al.* (1996)) rather than simply changes in atmospheric precipitation.

The proxies representing the aquatic system of Lake Kotokel reveal a more complex pattern of changes than could be seen in the terrestrial vegetation (i.e. biome scores and pollen PCA axis 1), in line with the supposedly higher sensitivity of the lake to direct and indirect impacts of climate change. The chironomid PCA axis 1 (Fig. 9H) reveals a rapid lake-level rise after *c.* 23.4 cal. ka BP, supporting the turn to a wetter climate, which was inferred from the pollen data (Fig. 9A, C, H). The C/N ratio (Fig. 9D) and *Pediastrum* percentages (Fig. 9E) appear to change in concert, suggesting their strong dependence on the water depth, which, in turn, is controlled by variations in precipitation and temperature. A visibly negative relationship between the higher C/N and *Pediastrum* values and the minima in the atmospheric precipitation curve (Fig. 9B) supports this interpretation. Furthermore, both the *Pediastrum* variations and the changes in ostracod and chironomid assemblage composition (Fig. 9G, H) suggest that the phase between *c.* 22.6 and 22.0 cal. ka BP was the deepest lake phase of the entire interval in line with the relatively moist environments suggested by the terrestrial proxies (Fig. 9A–C). The pollen PCA axis 2 (Fig. 9F) explains 29% of the variation and suggests a moderate (although still noticeable) response of the pollen composition at the KTK10 coring site to the changes in the littoral vegetation represented mainly by the pollen of Ranunculaceae. Two distinct peaks in the second PCA axis (and in Ranunculaceae percentages) appear within the earliest (driest) and the latest (wettest) phase derived from the different proxies. This feature possibly implies substantial lake-level fluctuations within these phases, as discussed above.

#### *Driving factors and mechanisms of the regional climate changes*

The strong relationship between the terrestrial environments (i.e. vegetation cover) and the aquatic system suggests climatic change to be the common underlying forcing factor, as demonstrated by limnological studies (e.g. Lotter & Anderson 2012; Hildebrandt *et al.* 2015), although diverse lacustrine and terrestrial system responses to deglacial warming have also been reported (e.g.

Wilson *et al.* 2015; Shala *et al.* 2017), preventing simple universal interpretations.

The present-day (i.e. ‘interglacial’) climate in the study area is mainly controlled by the westerly flow active through the whole year, while the thermal Asian anticyclone predominates during the colder half of the year and cyclonic activity along the Mongolian branch of the Polar front represents the summer period (Alpat’ev *et al.* 1976). The proxy-based reconstructions and model simulations (Kageyama *et al.* 2001; Hubberten *et al.* 2004; Andreev *et al.* 2011) suggest a much colder and drier than present LGM climate, which caused a virtual disappearance of the continuous temperate-boreal forest belt in the middle/high latitudes of Eurasia (Prentice & Jolly 2000; Williams *et al.* 2011). LGM annual temperatures about 20–25 °C colder than those of today, amplitudes of rapid temperature shifts as high as 8–10 °C, and annual precipitation up to three times lower than that of the modern value are reconstructed from the GRIP ice-core  $\delta^{18}\text{O}$  record for the summit of the Greenland Ice Sheet (Johnsen *et al.* 2001). Although proxy-derived and model-simulated temperature and precipitation anomalies may vary between different approaches (e.g. Leipe *et al.* 2015; Igarashi 2016) and study regions within northern Eurasia, there is basic agreement on two key points. Firstly, the reconstructed decrease in precipitation was strongly related to the changes in atmospheric circulation patterns (i.e. weaker moisture supply) due to the global ice-cover expansion and major lowering of the ocean level. Secondly, the LGM temperature and precipitation decrease was markedly greater in winter than in summer (e.g. Tarasov *et al.* 1999; Kageyama *et al.* 2001; Melles *et al.* 2012).

Quantitative climatic reconstructions for the Lake Baikal region are scarce and mainly refer to pollen records. Expert-estimated absolute values for the area around Lake Kotokel were reported by Shichi *et al.* (2009). They suggested annual precipitation of <250 mm and a mean January temperature dropping down to –32 °C during the LGM period. This estimate corroborates the pollen-based precipitation reconstruction for the study area based on an extensive modern pollen–climate dataset (Tarasov *et al.* 2005, 2017; Fig. 9B) and reflects globally cold and arid LGM climate conditions seen in proxy records and model simulations (e.g. Johnsen *et al.* 2001; Kageyama *et al.* 2001). Whilst much colder and drier than present LGM winters are generally accepted, the reconstructions of summer temperatures raise debates amongst scientists working in central and southern Siberia. Pollen-based interpretations are less conclusive, mainly because of the absence of temperature-sensitive tree pollen, the low taxonomic level of herbaceous taxa identification, and the large tolerance of the steppe biome to temperature changes (Kaplan *et al.* 2003). Tarasov *et al.* (1999) attempted to reconstruct mean temperatures of the warmest month (MTWM) using the best modern analogue and biomization approaches applied to the LGM pollen spectra from

the mid-latitude belt of northern Eurasia. The results revealed MTWM close to modern values (12–15 °C), with reconstruction uncertainties of  $\pm 3$  °C, at several sites from Siberia, Mongolia, and around Lake Baikal. Using a detailed record of plant macrofossils from the high Arctic site Mamontovy Khayata in the Lena River delta, Kienast *et al.* (2005) reconstructed an extremely continental, arid LGM climate with winters colder and summers distinctly warmer than at present. Their hypothesis is based on the similarity of the LGM vegetation composition to modern mosaic vegetation in the relict steppe areas of eastern Siberia, north and northeast of Lake Baikal. This reconstruction finds further support from the current study from Lake Kotokel. The high abundance of *Propylacanthus paradoxus* in the upper part of the KTK10 chironomid record (Fig. 7) provides strong evidence that the water temperature near the bottom of the lake reached at least 19 °C in summer between *c.* 23.4 and 22.0 cal. ka BP (cf. the present-day mean July air temperature is 15.4 °C). Indeed, similar or higher than present summer temperatures (and hence higher evaporation) in combination with lower than present precipitation and much colder winters with extremely thin snow cover would better explain the treeless productive steppe and meadow vegetation and associated rich herbivorous and predator fauna around Lake Baikal and in the vast regions of Siberia during the LGM suggested by a number of botanical (Kienast *et al.* 2005; Bezrukova *et al.* 2010; Müller *et al.* 2010), zoological (Pavelková Řičánková *et al.* 2014), archaeological (Fiedel & Kuzmin 2007), and DNA (Willerslev *et al.* 2014) records.

The synchronicity of East Asian and North Atlantic climate oscillations is shown by the correlation of isotope records from Greenland ice-cores with a stalagmite record from China (Wang *et al.* 2001). Magnetic susceptibility data from the Continent Ridge core of Lake Baikal indicate a rough correlation with events in the GISP2 ice-core, with the coldest period dated to *c.* 26–23 cal. ka BP (Boës *et al.* 2005). The detailed sedimentary record of climatic events from the Lake Baikal BDP-93-2 core (Prokopenko *et al.* 2001) and century-scale pollen record from the Lake Kotokel KTK2 core recognize distinct environmental changes during the last glacial interval that can be correlated to the Heinrich Events and the Greenland Interstadials recorded in the North Atlantic region (Johnsen *et al.* 2001; Svensson *et al.* 2008). The latter correlations suggest that the climatic teleconnection between the Lake Baikal region in central Eurasia and the North Atlantic region was not interrupted even during the coldest and driest interval of the Late Pleistocene (Bezrukova *et al.* 2010).

The Lake Kotokel proxies summarized in Fig. 9A–H facilitate comparison of the decadal/multidecadal-scale records representing terrestrial and aquatic environments in the study area with the proxies representing past climate variability in the North Atlantic and Northwest Pacific regions (Fig. 9I–K) during the 24–22 cal. ka BP interval in focus. Visual comparison of the Hulu Cave

stalagmite record of the East Asian monsoon (Wang *et al.* 2001; Fig. 9I) demonstrates surprisingly good correspondence of the major peaks in the  $\delta^{18}\text{O}$  curve *c.* 23.3 and *c.* 22.4 cal. ka BP (reflecting strengthening of the summer monsoon circulation) with the two major phases of increased precipitation around Lake Kotokel (Fig. 9B). The major drop in the GISP2  $\text{K}^+$  record from Greenland by 23.4 cal. ka BP (Mayewski *et al.* 1997) indicates a weaker Siberian high and a slightly warmer winter climate over Eurasia. The onset of hemispherically warmer conditions after *c.* 23.3 cal. ka BP and decadal/multidecadal-scale climatic variability documented in the  $\delta^{18}\text{O}$  NGRIP record (Svensson *et al.* 2008; Fig. 9J) can be traced in the analysed proxies from Lake Kotokel. It is worth mentioning that the numerous oscillations in the NGRIP temperature record corroborate changes in pollen-derived precipitation (Fig. 9B) and *Pediastrum*-inferred water depth (Fig. 9E). This suggests that climate-driven changes in effective moisture (and regional water balance) were the main forcing factor, which controlled terrestrial and aquatic environments in the study area and probably in the broader region of central Eurasia between 24 and 22 cal. ka BP.

## Conclusions

In sum, all proxies stored in the Lake Kotokel sedimentary archive demonstrate qualitatively and quantitatively distinct changes, indicating complex responses of the terrestrial and aquatic environments to the regional climate changes, as shown in the discussion above. Based on the present results, the regional climatic conditions between 24 and 22 cal. ka BP, i.e. during the global LGM interval, may be divided into three phases: a driest phase (*c.* 24.0–23.4 cal. ka BP) with low precipitation, high summer evaporation, and low lake levels and a phase (*c.* 22.6–22.0 cal. ka BP) of relatively high precipitation (and moisture availability) and relatively high lake levels, which are separated from each other by a transitional phase of unstable conditions (*c.* 23.4–22.6 cal. ka BP). During the driest phase, there is also evidence for short-term variations in atmospheric precipitation and substantial lake-level fluctuations. Our results also contribute to clarifying the regional LGM summer thermal conditions, which are still under debate. The findings advocate for at least 3.5 °C higher than present summer temperatures paralleled by increased levels of available moisture that were reached after the transitional phase (*c.* 22.6 cal. ka BP) identified in this study. Progressively warmer and wetter conditions following the end of the driest phase (after *c.* 23.4 cal. ka BP) are well in line with isotope data from Greenland ice-cores showing that teleconnections between central Eurasia and the North Atlantic continued through the LGM. Given the precipitation reconstructions, far-distant linkages are also indicated with the Northwest Pacific region. Moreover, it appears that environmental conditions during the LGM in central

Eurasia were mainly controlled by the interplay of much colder winter temperatures, relatively high summer temperatures, and varying levels of humidity.

*Acknowledgements.* – The research on Lake Kotokel greatly benefited from the international ‘Bridging Eurasia’ Research Initiative supported by the Center for International Cooperation at the Freie Universität Berlin (FUB), the German Archaeological Institute (DAI) and the Baikal-Hokkaido Archaeology Project. P. Tarasov and S. Müller acknowledge financial support from the German Research Foundation (DFG; grants TA 540/4, TA 540/5 and MU 3181/1) and S. Kostrova and E. Bezrukova extend their thanks to the State Research Program of the Institute of Geochemistry (Irkutsk) via the Project IX.127.1. (0350-2016-0026) and the Russian Science Foundation (RSF) grant no. 16-17-10079. The authors are grateful to Sergey Krivonogov (Institute of Geology and Mineralogy, Novosibirsk), Mayke Wagner (DAI), Frank Riedel and Annette Kossler (both FUB), and Tengwen Long (University of Nottingham Ningbo) for various help and valuable consultations during this project. We extend our thanks to Bernd Wagner, Finn Viehberg, and the anonymous reviewer for their helpful advice, which led to improvements in this paper.

## References

- Alpat'ev, A. M., Arkhangel'skii, A. M., Podoplelov, N. Y. & Stepanov, A. Y. 1976: *Fizicheskaya Geografiya SSSR (Aziatskaya Chast')*. 359 pp. Vysshaya Shkola, Moscow (in Russian).
- Andersen, T., Ekrem, T. & Cranston, P. S. (eds.) 2013: Chironomidae of the Holarctic Region. Keys and diagnoses – Larvae. *Insect Systematics and Evolution, Supplement 66*, 1–571.
- Andreev, A. A., Schirrmeister, L., Tarasov, P. E., Ganopolski, A., Brovkin, V., Siebert, C., Wetterich, S. & Hubberten, H.-W. 2011: Vegetation and climate history in the Laptev Sea region (Arctic Siberia) during Late Quaternary inferred from pollen records. *Quaternary Science Reviews 30*, 2182–2199.
- Bennett, K. D. 1996: Determination of the number of zones in a biostratigraphical sequence. *New Phytologist 132*, 155–170.
- Bennett, K. D. 2009: *Documentation for Pscimpoll 4.27 and Pscomb 1.03. C Programs for Plotting and Analyzing Pollen Data*. The 14Chrono Centre, Archaeology and Palaeoecology, Queen's University of Belfast, Belfast.
- Bennion, H. 1994: A diatom-phosphorus transfer function for shallow, eutrophic ponds in southeast England. *Hydrobiologia 275*, 391–410.
- Bezrukova, E. V., Tarasov, P. E., Solovieva, N., Krivonogov, S. K. & Riedel, F. 2010: Last glacial–interglacial vegetation and environmental dynamics in southern Siberia: chronology, forcing and feedbacks. *Palaeogeography, Palaeoclimatology, Palaeoecology 296*, 185–198.
- Birks, H. J. B. & Gordon, A. D. 1985: The analysis of pollen stratigraphical data: zonation. In Birks, H. J. B. & Gordon, A. D. (eds.): *Numerical Methods in Quaternary Pollen Analysis*, 47–90. Academic Press, London.
- Boës, X., Piotrowska, N. & Fagel, N. 2005: High-resolution diatom/clay record in Lake Baikal from grey scale, and magnetic susceptibility over Holocene and Termination I. *Global and Planetary Change 46*, 299–313.
- ter Braak, C. J. F. & Šmilauer, P. 2012: *Canoco Reference Manual and User's Guide: Software for Ordination (version 5.0)*. Microcomputer Power, Ithaca.
- Brodersen, K. P. & Lindegaard, C. 1997: Significance of subfossil chironomid remains in classification of shallow lakes. *Hydrobiologia 342/343*, 125–132.
- Brodersen, K. P. & Quinlan, R. 2006: Midges as palaeoindicators of lake productivity, eutrophication and hypolimnetic oxygen. *Quaternary Science Reviews 25*, 1995–2012.
- Brodersen, K. P., Pedersen, O., Lindegaard, C. & Hamburger, K. 2004: Chironomids (Diptera) and oxy-regulatory capacity: an experimental approach to paleolimnological interpretation. *Limnology and Oceanography 49*, 1549–1559.
- Bronk Ramsey, C. 1995: Radiocarbon calibration and analysis of stratigraphy: the OxCal program. *Radiocarbon 37*, 425–430.
- Brooks, S. J., Langdon, P. G. & Heiri, O. 2007: *The Identification and Use of Palaearctic Chironomidae Larvae in Palaeoecology*. 276 pp. Quaternary Research Association, London.
- Burkett, V. R., Wilcox, D. A., Stottleyer, R., Barrow, W., Fagre, D., Baron, J., Price, J., Nielsen, J. L., Allen, C. D., Peterson, D. L., Ruggerone, G. & Doyle, T. 2005: Nonlinear dynamics in ecosystem response to climatic change: case studies and policy implications. *Ecological Complexity 2*, 357–394.
- Clark, U. C., Dyke, A. S., Shakun, J. D., Carlson, A. E., Clark, J., Wohlfarth, B., Mitrovica, J. X., Hostetler, S. W. & McCabe, A. M. 2009: The last glacial maximum. *Science 325*, 710–714.
- Decrouy, L., Vennemann, T. W. & Ariztegui, D. 2011: Controls on ostracod valve geochemistry: part 2. Carbon and oxygen isotope compositions. *Geochimica et Cosmochimica Acta 75*, 7380–7399.
- DeFries, R. S., Hansen, M. C., Townshend, J. R. G., Janetos, A. C. & Loveland, T. R. 2000: A new global 1-km dataset of percentage tree cover derived from remote sensing. *Global Change Biology 6*, 247–254.
- Demske, D., Tarasov, P. E., Leipe, C., Kotlia, B. S., Joshi, L. M. & Long, T. 2016: Record of vegetation, climate change, human impact and retting of hemp in Garhwal Himalaya (India) during the past 4600 years. *The Holocene 26*, 1661–1675.
- Dierßen, K. & Dierßen, B. 1996: *Vegetation Nordeuropas*. 832 pp. Eugen Ulmer, Stuttgart.
- Dolukhanov, P. M., Shukurov, A. M., Tarasov, P. E. & Zaitseva, G. I. 2002: Colonization of Northern Eurasia by modern humans: radiocarbon chronology and environment. *Journal of Archaeological Science 29*, 593–606.
- Fan, Y., Chen, J., Shirkey, G., John, R., Wu, S. R., Park, H. & Shao, C. 2016: Applications of structural equation modeling (SEM) in ecological studies: an updated review. *Ecological Processes 5*, 19. <https://doi.org/10.1186/s13717-016-0063-3>.
- Fedotov, A. P., Vorobyeva, S. S., Vershinin, K. E., Nurgaliev, D. K., Enushchenko, I. V., Krapivina, S. M., Tarakanova, K. V., Ziborova, G. A., Yassonov, P. G. & Borissov, A. S. 2012: Climate changes in East Siberia (Russia) in the Holocene based on diatom, chironomid and pollen records from the sediments of Lake Kotokel. *Journal of Paleolimnology 47*, 617–630.
- Fiedel, S. J. & Kuzmin, Y. V. 2007: Radiocarbon date frequency as an index of intensity of paleolithic occupation of Siberia: did humans react predictably to climate oscillations? *Radiocarbon 49*, 741–756.
- Galaziy, G. I. (ed.) 1993: *Baikal Atlas*. 160 pp. Federal Agency for Geodesy and Cartography of Russia, Moscow (in Russian).
- Ganopolski, A., Calov, R. & Claussen, M. 2010: Simulation of the last glacial cycle with a coupled climate ice-sheet model of intermediate complexity. *Climate of the Past 6*, 229–244.
- Grace, J. B. 2006: *Structural Equation Modeling and the Study of Natural Systems*. 361 pp. Cambridge University Press, Cambridge.
- von Grafenstein, U., Erlernkeuser, H. & Trimborn, P. 1999: Oxygen and carbon isotopes in modern fresh-water ostracod valves: assessing vital offsets and autecological effects of interest for palaeoclimate studies. *Palaeogeography, Palaeoclimatology, Palaeoecology 148*, 133–152.
- Grimm, E. C. 2004: *TGView Software*. Illinois State Museum, Springfield.
- Guthrie, R. D. 2001: Origin and causes of the mammoth steppe: a story of cloud cover, woolly mammal tooth pits, buckles, and inside-out Beringia. *Quaternary Science Reviews 20*, 549–574.
- Heiri, O. & Lotter, A. F. 2001: Effect of low count sums on quantitative environmental reconstructions: an example using subfossil chironomids. *Journal of Paleolimnology 26*, 343–350.
- Hilbert, D. W. 2002: Non-linear systems. In Munn, T., Mooney, H. A. & Canadell J. G. (eds.): *Encyclopedia of Global Environmental Change. Volume 2: The Earth System: Biological and Ecological Dimensions of Global Environmental Change*, 450–455. John Wiley and Sons Ltd., Chichester.
- Hilbig, W. 1995: *The Vegetation of Mongolia*. 258 pp. SPB Academic Publishing, Amsterdam.
- Hildebrandt, S., Müller, S., Kalugin, I. A., Dar'in, A. V., Wagner, M., Rogozin, D. Y. & Tarasov, P. E. 2015: Tracing the North Atlantic decadal-scale climate variability in a late Holocene pollen record from southern Siberia. *Palaeogeography, Palaeoclimatology, Palaeoecology 426*, 75–84.

- Hofmann, W. 1988: The significance of chironomid analysis (Insecta: Diptera) for paleolimnological research. *Palaeogeography, Palaeoclimatology, Palaeoecology* 62, 501–509.
- Hofmann, W. 1998: Cladocerans and chironomids as indicators of lake level changes in north temperate lakes. *Journal of Paleolimnology* 19, 55–62.
- Hubberten, H.-W., Andreev, A., Astakhov, V. I., Demidov, I., Dowdeswell, J. A., Henriksen, M., Hjort, C., Houmark-Nielsen, M., Jakobsson, M., Kuzmina, S., Larsen, E., Lunkka, J. P., Lyså, A., Mangerud, J., Möller, P., Saarnisto, M., Schirmermeister, L., Sher, A. V., Siegert, C., Siegert, M. J. & Svendsen, J. I. 2004: The periglacial climate and environment in northern Eurasia during the last glaciation. *Quaternary Science Reviews* 23, 1333–1357.
- Igarashi, Y. 2016: Vegetation and climate during the LGM and the last deglaciation on Hokkaido and Sakhalin Islands in the northwest Pacific. *Quaternary International* 425, 28–37.
- IPCC 2014: Climate Change 2014: Synthesis Report. Contribution of Working Groups I, II and III to the Fifth Assessment Report of the Intergovernmental Panel on Climate Change (Core Writing Team, R. K. Pachauri & L. A. Meyer (eds.)). IPCC, Geneva.
- Jarvis, A., Reuter, H. I., Nelson, A. & Guevara, E. 2008: *Hole-filled SRTM for the globe Version 4*, available from the CGIAR-CSI SRTM 90m Database. Available at: <http://srtm.csi.cgiar.org>.
- Johnsen, S. J., Dahl-Jensen, D., Gundestrup, N., Steffensen, J. P., Clausen, H. B., Miller, H., Masson-Delmotte, V., Sveinbjörnsdóttir, A. E. & White, J. 2001: Oxygen isotope and palaeotemperature records from six Greenland ice-core stations: Camp Century, Dye-3, GRIP, GISP2, Renland and NorthGRIP. *Journal of Quaternary Science* 16, 299–307.
- Juggins, S. 2007: *C2 User Guide: Software for Ecological and Palaeoecological Data Analysis and Visualisation*. 73 pp. University of Newcastle, Newcastle.
- Kageyama, M., Peyron, O., Pinot, S., Tarasov, P., Guiot, J., Joussaume, S., Ramstein, G. & PMIP Participating Groups 2001: The Last Glacial Maximum climate over Europe and western Siberia: a PMIP comparison between models and data. *Climate Dynamics* 17, 23–43.
- Kaplan, J. O., Bigelow, N. H., Prentice, I. C., Harrison, S. P., Bartlein, P. J., Christensen, T. R., Cramer, W., Matveyeva, N. V., McGuire, A. D., Murray, D. F., Razzhivin, V. Y., Smith, B., Walker, D. A., Anderson, P. M., Andreev, A. A., Brubaker, L. B., Edwards, M. E. & Lozhkin, A. V. 2003: Climate change and Arctic ecosystems: 2. Modeling, paleodata-model comparisons, and future projections. *Journal of Geophysical Research* 108, 8171. <https://doi.org/10.1029/2002jd002559>.
- Karabanov, E., Williams, D., Kuzmin, M., Sideleva, V., Khursevich, G., Prokopenko, A., Solotchina, E., Tkachenko, L., Fedenya, S. & Kerber, E. 2004: Ecological collapse of Lake Baikal and Lake Hovsgol ecosystems during the Last Glacial and consequences for aquatic species diversity. *Palaeogeography, Palaeoclimatology, Palaeoecology* 209, 227–243.
- Keatings, K. W., Holmes, J. A. & Heaton, T. H. E. 2006: Effects of pre-treatment on ostracod valve chemistry. *Chemical Geology* 235, 250–261.
- Keddy, P. A. & Reznicek, A. A. 1986: Great Lakes vegetation dynamics: the role of fluctuating water levels and buried seeds. *Journal of Great Lakes Research* 12, 25–36.
- Kienast, F., Schirmermeister, L., Siegert, C. & Tarasov, P. 2005: Palaeobotanical evidence for warm summers in the East Siberian Arctic during the last cold stage. *Quaternary Research* 63, 283–300.
- Kienast, F., Wetterich, S., Kuzmina, S., Schirmermeister, L., Andreev, A., Tarasov, P., Nazarova, L., Kossler, A., Frolova, L. & Kunitsky, V. V. 2011: Paleontological records indicate the occurrence of open woodlands in a dry inland climate at the present-day Arctic coast in western Beringia during the last interglacial. *Quaternary Science Reviews* 30, 2134–2159.
- Kock, N. 2015: *WarpPLS 5.0 User Manual*. 108 pp. ScriptWarp Systems, Laredo.
- Korde, N. V. 1968: *Mezozoiskie i Kainozoiskie Ozera Sibiri*. 261 pp. Nauka, Moscow.
- Kornijów, R. & Halkiewicz, A. 2007: Are the larvae of *Prosilocerus lacustris* Kieffer 1923 (Diptera: Chironomidae) favoured by nutrient-rich lakes? *Aquatic Insects* 29, 187–194.
- Kossler, A. 2010: Faunen und Floren der limnisch-telmatischen Schichtenfolge des Paddenluchs (Brandenburg, Rüdersdorf) vom ausgehenden Weichselhochglazial bis ins Holozän). *Berliner Paläobiologische Abhandlungen* 11, 1–422.
- Kossler, A., Tarasov, P., Scholaut, G., Nakagawa, T., Marshall, M., Brauer, A., Staff, R., Bronk Ramsey, C., Bryant, C., Lamb, H., Demske, D., Gotanda, K., Haraguchi, T., Yokoyama, Y., Yonenobu, H., Tada, R. & Suigetsu 2006 Project Members. 2011: Onset and termination of the late-glacial climate reversal in the high-resolution diatom and sedimentary records from the annually laminated SG06 core from Lake Suigetsu, Japan. *Palaeogeography, Palaeoclimatology, Palaeoecology* 306, 103–115.
- Kostrova, S. S., Meyer, H., Chaplign, B., Kossler, A., Bezrukova, E. V. & Tarasov, P. E. 2013: Holocene oxygen isotope record of diatoms from Lake Kotokel (southern Siberia, Russia) and its palaeoclimatic implications. *Quaternary International* 290–291, 21–34.
- Kostrova, S. S., Meyer, H., Chaplign, B., Tarasov, P. E. & Bezrukova, E. V. 2014: The last glacial maximum and late glacial environmental and climate dynamics in the Baikal region inferred from an oxygen isotope record of lacustrine diatom silica. *Quaternary International* 348, 25–36.
- Kurita, N., Yoshida, N., Inoue, G. & Chayanova, E. A. 2004: Modern isotope climatology of Russia: a first assessment. *Journal of Geophysical Research* 109, D03102. <https://doi.org/10.1029/2003JD003404>.
- Larocque-Tobler, I. 2014: The Polish sub-fossil chironomids. *Palaeontologia Electronica* 17, 1; 3A, 28 pp.
- Leipe, C., Nakagawa, T., Gotanda, K., Müller, S. & Tarasov, P. E. 2015: Late Quaternary vegetation and climate dynamics at the northern limit of the East Asian summer monsoon and its regional and global-scale controls. *Quaternary Science Reviews* 116, 57–71.
- Leng, M. J. & Marshall, J. D. 2004: Palaeoclimate interpretation of stable isotope data from lake sediment archives. *Quaternary Science Reviews* 23, 811–831.
- Li, Y., Rioual, P., Shen, J. & Xiao, X. 2015: Diatom response to climatic and tectonic forcing of a palaeolake at the southeastern margin of the Tibetan Plateau during the late Pleistocene, between 140 and 35 ka BP. *Palaeogeography, Palaeoclimatology, Palaeoecology* 436, 123–134.
- Lisiecki, L. E. & Raymo, M. E. 2005: A Pliocene-Pleistocene stack of 57 globally distributed benthic  $^{18}\text{O}$  records. *Paleoceanography* 20, PA1003. <https://doi.org/10.1029/2004pa001071>.
- Löffler, H. 1969: Recent and subfossil distribution of *Cytherissa lacustris* (Ostracoda) in Lake Constance. *Internationale Vereinigung für Theoretische und Angewandte Limnologie: Mitteilungen* 17, 240–251.
- Löffler, H. 1971: Daten zur subfossilen und lebenden Ostrakodenfauna in Wörthersee und Klopeinensee. *Carinthia II, Sonderheft* 31, 79–89.
- Lotter, A. F. & Anderson, N. J. 2012: Chapter 18: limnological responses to environmental changes at inter-annual to decadal time-scales. In Birks, H. J. B., Lotter, A. F., Juggins, S. & Smol, J. P. (eds.): *Tracking Environmental Change Using Lake Sediments, Volume 5*, 557–578. Springer, Dordrecht.
- Lotter, A. F. & Bigler, C. 2000: Do diatoms in the Swiss Alps reflect the length of ice cover? *Aquatic Sciences* 62, 125–141.
- Lotter, A. F., Pienitz, R. & Schmidt, R. 2010: Diatoms as indicators of environmental change in subarctic and alpine regions. In Smol, J. P. & Stoermer, E. F. (eds.): *The Diatoms: Applications for the Environmental and Earth Sciences*, 231–248. Cambridge University Press, Cambridge.
- Luoto, T. P. 2012: Spatial uniformity in depth optima of midges: evidence from sedimentary archives of shallow Alpine and boreal lakes. *Journal of Limnology* 71, 228–232.
- Lydolph, P. E. 1977: *Climates of the Soviet Union, World Survey of Climatology, Volume 7*. 443 pp. Elsevier Scientific Publishing Company, Amsterdam.
- Makarchenko, E. A. & Makarchenko, M. A. 2009: *Prosilocerus amurensis* sp.n. (Diptera, Chironomidae, Orthocladinae) from Amur River basin (Russian Far East). *Euroasian Entomological Journal* 8, 261–263.
- Mangerud, J., Gosse, J., Matiouchkov, A. & Dolvik, T. 2008: Glaciers in the Polar Urals, Russia, were not much larger during the Last Global Glacial Maximum than today. *Quaternary Science Reviews* 27, 1047–1057.

- Mayewski, P., Meeker, L. D., Twickler, M. S., Whitlow, S., Yang, Q. & Prentice, M. 1997: Major features and forcing of high latitude northern hemisphere circulation using a 110,000-year-long glacio-chemical series. *Journal of Geophysical Research* 102, 26345–26366.
- Meisch, C. 2000: *Freshwater Ostracoda of Western and Central Europe*. 522 pp. Spektrum Akademischer Verlag, Heidelberg.
- Melles, M., Brigham-Grette, J., Minyuk, P. S., Nowaczyk, N. R., Wennrich, V., DeConto, R. M., Anderson, P. M., Andreev, A. A., Coletti, A., Cook, T. L., Haltia-Hovi, E., Kukkonen, M., Lozhkin, A. V., Rosén, P., Tarasov, P., Vogel, H. & Wagner, B. 2012: 2.8 Million years of Arctic climate change from Lake El'gygytgyn, NE Russia. *Science* 337, 315–320.
- Meyers, P. A. & Ishiwatari, R. 1995: Organic matter accumulation records in lake sediments. In Lerman, A., Imboden, D. M. & Gat, J. R. (eds.): *Physics and Chemistry of Lakes*, 279–328. Springer, Berlin.
- Meyers, P. A. & Teranes, J. L. 2001: Sediment organic matter. In Last, W. M. & Smol, J. P. (eds.): *Tracking Environmental Changes Using Lake Sediment, Volume 2: Physical and Geochemical Methods*, 239–270. Kluwer Academic, Dordrecht.
- Molozhnikov, V. N. 1986: *Rastitel'nye Soobshchestva Pribaikal'ya*. 272 pp. Nauka, Novosibirsk.
- Mortsch, L. D. 1998: Assessing the impact of climate change on the Great Lakes shoreline wetlands. *Climatic Change* 40, 391–416.
- Müller, S., Tarasov, P. E., Andreev, A. A., Tütken, T., Gartz, S. & Diekmann, B. 2010: Late Quaternary vegetation and environments in the Verkhoyansk Mountains region (NE Asia) reconstructed from a 50-kyr fossil pollen record from Lake Billyakh. *Quaternary Science Reviews* 29, 2071–2086.
- Müller, S., Tarasov, P. E., Hoelzmann, P., Bezrukova, E. V., Kossler, A. & Krivonogov, S. K. 2014: Stable vegetation and environmental conditions during the Last Glacial Maximum: new results from Lake Kotokel (Lake Baikal region, southern Siberia, Russia). *Quaternary International* 348, 14–24.
- Nazarova, L., Herzschuh, U., Wetterich, S., Kumke, T. & Pestryakova, L. 2011: Chironomid-based inference models for estimating mean July air temperature and water depth from lakes in Yakutia, northeastern Russia. *Journal of Paleolimnology* 45, 57–71.
- Newrkla, P. 1985: Respiration of *Cytherissa lacustris* (Ostracoda) at different temperatures and its tolerance towards temperature and oxygen concentration. *Oecologia* 67, 250–254.
- Pankratova, V. Y. 1983: *Larvae and Pupae of Non-Biting Midges of the Subfamilies Chironominae (Diptera, Chironomidae = Tendipedidae) of the USSR Fauna*. 296 pp. Nauka, Leningrad.
- Pavelková Řičánková, V., Robovský, J. & Riegert, J. 2014: Ecological structure of recent and last glacial mammalian faunas in Northern Eurasia: the case of Altai-Sayan refugium. *PLoS ONE* 9, e85056, <https://doi.org/10.1371/journal.pone.0085056>.
- Petit, R. J., Hu, F. S. & Dick, C. W. 2008: Forests of the past: a window to future changes. *Science* 320, 1450–1452.
- Petrova, N. A., Klishko, O. K., Zelentsov, N. I. & Chubareva, L. A. 2003: Primary description of polytene chromosomes, larval morphology and biology of two species of the genus *Propislocerus* (Diptera, Chironomidae, Orthocladinae). *Proceedings of the Russian Entomological Society* 74, 33–50 (in Russian).
- Powell, S. 1976: *Einige Aspekte der Beziehung zwischen Sedimenteigenschaften und der Fortbewegung benthischer Süßwasserostrakoden, mit spezieller Berücksichtigung der Cytherissa lacustris (Sars)*. Ph.D. thesis, University of Wien, 122 pp.
- Prentice, C. I., Guiot, J., Huntley, B., Jolly, D. & Cheddadi, R. 1996: Reconstructing biomes from palaeoecological data: a general method and its application to European pollen data at 0 and 6 ka. *Climate Dynamics* 12, 185–194.
- Prentice, I. C., Jolly, D. & 6000 BIOME Participants. 2000: Mid-Holocene and glacial maximum vegetation geography of the northern continents and Africa. *Journal of Biogeography* 27, 507–519.
- Prokopenko, A. A., Karabanov, E. B., Williams, D. F., Kuzmin, M. I., Khursevich, G. K. & Gvozdkov, A. A. 2001: The detailed record of climatic events during the past 75,000 yrs BP from the Lake Baikal drill core BDP-93-2. *Quaternary International* 80–81, 59–68.
- Reimer, P. J., Bard, E., Bayliss, A., Beck, J. W., Blackwell, P. G., Bronk Ramsey, C., Buck, C. E., Cheng, H., Edwards, R. L., Friedrich, M., Grootes, P. M., Guilderson, T. P., Haflidason, H., Hajdas, I., Hatté, C., Heaton, T. J., Hoffmann, D. L., Hogg, A. G., Hughen, K. A., Kaiser, K. F., Kromer, B., Manning, S. W., Niu, M., Reimer, R. W., Richards, D. A., Scott, E. M., Southon, J. R., Staff, R. A., Turney, C. S. M. & van der Plicht, J. 2013: IntCal13 and MARINE13 radiocarbon age calibration curves 0–50,000 years cal BP. *Radiocarbon* 55, 1869–1887.
- Sæther, O. A. & Wang, X. 1996: Revision of the genus *Propislocerus* Kieffer, 1923 (=Tokunagayusurika Sasa) (Diptera: Chironomidae). *Entomologica Scandinavica* 27, 441–479.
- Schulz, M. & Paul, A. 2015: *Integrated Analysis of Interglacial Climate Dynamics (INTERDYNAMIC)*, Series: *Springer Briefs in Earth System Sciences*. 139 pp. Springer, Heidelberg.
- Shala, S., Helmens, K. F., Luoto, T. P., Salonen, J. S., Väiliranta, M. & Weckström, J. 2017: Comparison of quantitative Holocene temperature reconstructions using multiple proxies from a northern boreal lake. *The Holocene* 27, 1745–1755.
- Shichi, K., Takahara, H., Krivonogov, S. K., Bezrukova, E. V., Kashiwaya, K., Takehara, A. & Nakamura, T. 2009: Late Pleistocene and Holocene vegetation and climate records from Lake Kotokel, central Baikal region. *Quaternary International* 205, 98–110.
- Svendsen, J. I., Alexanderson, H., Astakhov, V. I., Demidov, I., Dowdeswell, J. A., Funder, S., Gataullin, V., Henriksen, M., Hjort, C., Houmark-Nielsen, M., Hubberten, H.-W., Ingólfsson, O., Jakobsson, M., Kjær, K. H., Larsen, E., Lokrantz, H., Lunkka, J. P., Lyså, A., Mangerud, J., Matiouchkov, A., Murray, A., Möller, P., Niessen, F., Nikolskaya, O., Polyak, L., Saarnisto, M., Siegert, C., Siegert, M. J., Spielhagen, R. F. & Stein, R. 2004: Late Quaternary ice sheet history of northern Eurasia. *Quaternary Science Reviews* 23, 1229–1271.
- Svensson, A., Andersen, K. K., Bigler, M., Clausen, H. B., Dahl-Jensen, D., Davies, S. M., Johnsen, S. J., Muscheler, R., Parrenin, F., Rasmussen, S. O., Rothlisberger, R., Seierstad, I., Steffensen, J. P. & Vinther, B. M. 2008: A 60,000 year Greenland stratigraphic ice core chronology. *Climate of the Past* 4, 47–57.
- Tarasov, P. E., Bezrukova, E. V. & Krivonogov, S. K. 2009: Late glacial and Holocene changes in vegetation cover and climate in southern Siberia derived from a 15 kyr long pollen record from Lake Kotokel. *Climate of the Past* 5, 73–84.
- Tarasov, P. E., Bezrukova, E. V., Müller, S., Kostrova, S. S. & White, D. 2017: Chapter 2: climate and vegetation history. In Losey, R. J. & Nomokonova, T. (eds.): *Holocene Zooarchaeology of Cis-Baikal, Archaeology in China and East Asia* 6, 15–26. Philipp von Zabern, Darmstadt.
- Tarasov, P., Granoszewski, W., Bezrukova, E., Brewer, S., Nita, M., Abzaeva, A. & Oberhänsli, H. 2005: Quantitative reconstruction of the Last Interglacial vegetation and climate based on the pollen record from Lake Baikal, Russia. *Climate Dynamics* 25, 625–637.
- Tarasov, P. E., Peyron, O., Guiot, J., Brewer, S., Volkova, V. S., Bezusko, L. G., Dorofeyuk, N. I., Kvavadze, E. V., Osipova, I. M. & Panova, N. K. 1999: Last Glacial Maximum climate of the Former Soviet Union and Mongolia reconstructed from pollen and plant macrofossil data. *Climate Dynamics* 15, 227–240.
- Vipper, P. B. 1968: Vzaimodeistvie lesa i stepi v gornykh usloviyakh yugo-zapadnogo Zabaikalya. *Botanicheskii Zhurnal* 53, 491–504.
- Walker, I. R. 2001: Midges: Chironomidae and related Diptera. In Smol, J. P., Birks, H. J. B. & Last, W. M. (eds.): *Tracking Environmental Change Using Lake Sediments, Volume 4: Zoological indicators*, 43–66. Kluwer Academic Press, Dordrecht.
- Wang, Y. J., Cheng, H., Edwards, R. L., An, Z. S., Wu, J. Y., Shen, C.-C. & Dorale, J. A. 2001: A high-resolution absolute-dated Late Pleistocene Monsoon record from Hulu Cave, China. *Science* 294, 2345–2348.
- Willemslev, E., Davison, J., Moora, M., Zobel, M., Coissac, E., Edwards, M. E., Lorenzen, E. D., Vestergård, M., Gussarova, G., Haile, J., Craine, J., Gielly, L., Boessenkool, S., Epp, L. S., Pearson, P. B., Cheddadi, R., Murray, D., Bräthen, K. A., Yoccoz, N. B., Binney, H., Cruaud, C., Wincker, P., Goslar, T., Alsos, I. G., Bellemain, E., Brystant, A. K., Elven, R., Sønstebo, J. H., Murton, J., Sher, A., Rasmussen, M., Rønn, R., Mourier, T., Cooper, A., Austin, J., Möller, P., Froese, D., Zazula, G., Pompanon, F., Rioux, D., Niderkorn, V., Tikhonov, A., Savvinov, G., Roberts, R. G., MacPhee,

- R. D. E., Gilbert, M. T. P., Kjær, K. H., Orlando, L., Brochmann, C. & Taberlet, P. 2014: Fifty thousand years of Arctic vegetation and megafaunal diet. *Nature* 506, 47–51.
- Williams, J. W., Tarasov, P., Brewer, S. & Notaro, M. 2011: Late Quaternary variations in tree cover at the northern forest-tundra ecotone. *Journal of Geophysical Research* 116, G01017, <https://doi.org/10.1029/2010jg001458>.
- Wilson, G. P., Reed, J. M., Frogley, M. R., Hughes, P. D. & Tzedakis, P. C. 2015: Reconciling diverse lacustrine and terrestrial system response to penultimate deglacial warming in southern Europe. *Geology* 43, 819–822.
- Wold, S., Sjöström, M. & Eriksson, L. 2001: PLS-regression: a basic tool of chemometrics. *Chemometrics and Intelligent Laboratory Systems* 58, 109–130.
- Zhang, Y., Wünnemann, B., Bezrukova, E. V., Ivanov, E. V., Shchetnikov, A. A., Nourgaliev, D. & Levina, O. 2013: Basin morphology and seismic stratigraphy of Lake Kotokel, Baikal region, Russia. *Quaternary International* 290–291, 57–67.